

**Stochastic Simulation of the Generalized Lindblad
Master Equation
Discipline of Physics
School of Chemistry and Physics
University of KwaZulu-Natal**

Makhosonke H Thabethe

July 2016

As the candidate's supervisor. I have approved this dissertation for submission

Signed: _____ Name: _____ Date: _____

Signed: _____ Name: _____ Date: _____

Preface

The research contained in this dissertation was completed by the candidate while based in the Discipline of Physics, School of Chemistry and Physics of the College of Agriculture, Engineering and Science, University of KwaZulu-Natal, Durban, South Africa.

The contents of this work have not been submitted in any form to another university and, except where the work of others is acknowledged in the text, the results reported are due to investigations by the candidate.

Signed:

Date:

Declaration 1: Plagiarism

I, Makhosonke Henry Thabethe, declare that:

1. the research reported in this dissertation, except where otherwise indicated or acknowledged, is my original work;
2. this dissertation has not been submitted in full or in part for any degree or examination to any other university;
3. this dissertation does not contain other persons' data, pictures, graphs or other information, unless specifically acknowledged as being sourced from other persons;
4. this dissertation does not contain other persons' writing, unless specifically acknowledged as being sourced from other researchers. Where other written sources have been quoted, then:
 - a) their words have been re-written but the general information attributed to them has been referenced;
 - b) where their exact words have been used, their writing has been placed inside quotation marks, and referenced;
5. this dissertation does not contain text, graphics or tables copied and pasted from the Internet, unless specifically acknowledged, and the source being detailed in the dissertation and in the References sections.

Signed:

Date:

Abstract

Stochastic simulation of the generalized Lindblad equation for a specific model is performed. A two-state system that is coupled to a structured environment is studied as the model of interest. The environment consists of two energy bands with finite number of energy levels (N_1 and N_2) and level spacings $\delta\epsilon$. Depending on the coupling strength between the two-level system and the environment, the model can either be classified as Markovian or non-Markovian. In performing the time-convolutionless expansion, two master equations for the model are obtained which are of the generalized Lindblad form. These equations are stochastically unraveled revealing that the system can be described by two wave functions, $|\psi_1\rangle$ and $|\psi_2\rangle$ which evolve simultaneously. Monte Carlo wave-function simulations are performed to investigate the dynamics of the model, both in the weak and strong coupling regimes. These simulations are used to calculate both the ground and excited state populations and coherences of the system. Parameters $\delta\epsilon$, N_1 , and N_2 are varied interchangeably in the Monte Carlo code (written in Python language) to observe the relationship with the relaxation rates (γ). The populations and coherences of this model are then plotted for different values of $\delta\epsilon$, N_1 , and N_2 against time. Error bars are also plotted to show the statistics of the data for different values of $\delta\epsilon$, N_1 and N_2 . We consider as initial states, both pure and correlated states. For the pure state, the initial conditions were $|\psi_1(0)\rangle = |e\rangle$ and $|\psi_2(0)\rangle = |0\rangle$. In the correlated state, the initial conditions are dictated by population ratios (β) as $|\psi(0)\rangle = \beta|g\rangle + \sqrt{1-\beta}e^{i\phi}|e\rangle$. The significance of this condition is that both the upper and lower levels are populated at the same time.

Acknowledgements

I would like to thank my supervisors Dr. M. Moodley and Prof F. Petruccione for the time and energy they have devoted in supporting and guiding me for the duration of my masters research.

Contents

Preface	i
Declaration	ii
Abstract	iii
Acknowledgements	iv
Contents	v
List of Figures	vii
1 Introduction	1
2 Generalized master equation and its Stochastic unravelling	6
2.1 Projection Operator Technique	6
2.2 The Nakajima-Zwanzig projection operator technique	7
2.3 The time-convolutionless projection operator method	8
2.4 Structure of non-Markovian master equation	10
2.5 Unravelling the quantum master equation	12
3 Model and Time Convolutionless Approximation	15
3.1 Two level system	15
3.2 TCL expansion using the correlated projection superoperator	16

4	Stochastic wave-function simulations	20
4.1	Monte Carlo simulations	20
4.2	Monte Carlo code Flow Chart	25
5	Results and discussions	27
5.1	Pure state	27
5.1.1	Weak coupling results	28
5.1.2	Strong coupling results	35
5.2	Correlated state	42
5.2.1	Weak coupling results	43
5.2.2	Strong coupling results	47
6	Conclusions	50
	Appendices	51
A	Monte Carlo codes	52
A.1	Weak coupling for pure state	52
A.2	Strong coupling for pure state	57
A.3	Weak coupling for correlated state	65
A.4	Strong coupling for correlated state	70

List of Figures

1.1	Open Quantum system S interacting with the environment E	2
3.1	Two level system coupled to the environment [2].	15
4.1	Flow chart showing the Monte Carlo code.	26
5.1	The ground state population for $N_1 = N_2 = 200$ with $\lambda = 0.001$ and $\delta\epsilon = 0.31$	30
5.2	The ground state populations for variation of N_1 and N_2 with $\lambda = 0.001$ and $\delta\epsilon = 0.31$	30
5.3	The excited state populations for variation of N_1 and N_2 with $\lambda = 0.001$ and $\delta\epsilon = 0.31$	31
5.4	The ground state populations for variation of $\delta\epsilon$ with $N_1 = N_2 = 150$ and $\lambda = 0.001$	31
5.5	The excited state populations for variation of $\delta\epsilon$ with $N_1 = N_2 = 150$ and $\lambda = 0.001$	32
5.6	The ground state populations for variation of N_1 with $N_2 = 150$, $\lambda = 0.001$, and $\delta\epsilon = 0.31$	32
5.7	The excited state populations for variation of N_1 with $N_2 = 150$, $\lambda = 0.001$, and $\delta\epsilon = 0.31$	33
5.8	The ground state populations for variation of N_2 with $N_1 = 150$, $\lambda = 0.001$, and $\delta\epsilon = 0.31$	33

5.9	The excited state populations for variation of N_2 with $N_1 = 150$, $\lambda = 0.001$, and $\delta\epsilon = 0.31$	34
5.10	The ground state population for $N_1 = N_2 = 200$ with $\delta\epsilon = 0.31$, and $\lambda = 0.01$	37
5.11	The ground state populations for variation of N_1 and N_2 with $\delta\epsilon = 0.31$, and $\lambda = 0.01$	37
5.12	The excited state populations for variation of N_1 and N_2 with $\delta\epsilon = 0.31$, and $\lambda = 0.01$	38
5.13	The ground state populations for variation of $\delta\epsilon$ with $N_1 = N_2 = 150$, and $\lambda = 0.01$	38
5.14	The excited state populations for variation of $\delta\epsilon$ with $N_1 = N_2 = 150$, and $\lambda = 0.01$	39
5.15	The ground state populations for variation of N_1 with $N_2 = 150$, $\delta\epsilon = 0.31$, and $\lambda = 0.01$	39
5.16	The excited state populations for variation of N_1 with $N_2 = 150$, $\delta\epsilon = 0.31$, and $\lambda = 0.01$	40
5.17	The ground state populations for variation of N_2 with $N_1 = 150$, $\delta\epsilon = 0.31$, and $\lambda = 0.01$	40
5.18	The excited state populations for variation of N_2 with $N_1 = 150$, $\delta\epsilon = 0.31$, and $\lambda = 0.01$	41
5.19	The ground state population for the variation of energy levels $N_1 = N_2 = N$ with $\delta\epsilon = 0.31$, and $\lambda = 0.001$	45
5.20	The excited state population for the variation of number levels $N_1 = N_2 = N$ with $\delta\epsilon = 0.31$, and $\lambda = 0.001$	45
5.21	The coherences for $N_1 = N_2 = 100$ with $\delta\epsilon = 0.31$, and $\lambda = 0.001$	46
5.22	The coherences for the variation of number levels $N_1 = N_2 = N$ with $\delta\epsilon = 0.31$, and $\lambda = 0.001$	46
5.23	The ground state population for the variation of energy levels $N_1 = N_2 = N$ with $\delta\epsilon = 0.31$, and $\lambda = 0.001$	48

5.24	The excited state population for the variation of number levels $N_1 = N_2 = N$ with $\delta\epsilon = 0.31$, and $\lambda = 0.001$	48
5.25	The coherences for $N_1 = N_2 = 100$ with $\delta\epsilon = 0.31$, and $\lambda = 0.001$	49
5.26	The coherences for the variation of number levels $N_1 = N_2 = N$ with $\delta\epsilon =$ 0.31 , and $\lambda = 0.001$	49

Chapter 1

Introduction

A two level system is regarded as a core of all quantum technology devices which transfer information [1, 2]. However it is almost impossible to isolate the two level system with its surroundings which makes it to be an open quantum system [3, 4, 5]. An open quantum system is taken as a quantum mechanical system that interacts with the environment [4, 5]. This interaction results freely exchange information which affects the measurements of the observables that describe the dynamics of the system. An open quantum system provides a better approximation of reality and so therefore influence of the environment should always be taken into consideration [4, 6]. Figure 1.1 below shows subsystem S (in Hilbert space, \mathcal{H}_S) coupled in the environment E (in Hilbert space, \mathcal{H}_E).

To fully describe the dynamical evolution of an open quantum system, one defines an open system S and an environment E coupled to give a larger combined system $S + E$ (in Hilbert space, $\mathcal{H}_S \otimes \mathcal{H}_E$). The state of the system S evolves due to the interactions with environment E . The state of the system is described by the density operator $\rho_S \in \mathcal{H}_S$ which is defined as the operator that provides information about the quantum system. Similarly, $\rho_E \in \mathcal{H}_E$ describes the state of the environment. The full density matrix for the combined system and environment is described by $\rho \in \mathcal{H}_S \otimes \mathcal{H}_E$. The reduced density matrix of the system is obtained by taking the partial trace over the environmental degrees of freedom:

$$\rho_S(t) = tr_E \rho(t). \tag{1.1}$$

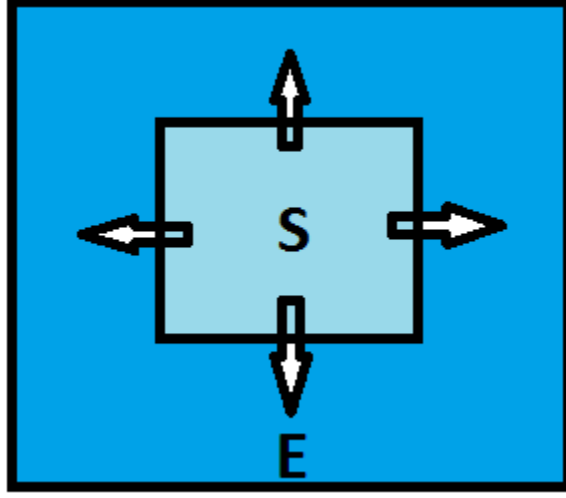


Figure 1.1: Open Quantum system S interacting with the environment E .

The starting point to derive the master equation for the system is by considering the Hamiltonian of the system, environment, and system-environment interaction

$$H = H_S + H_E + H_I. \quad (1.2)$$

Here H_S represents the Hamiltonian for the system, H_E is the Hamiltonian for the environment, and H_I is the interaction Hamiltonian. Introducing an operator that is transformed into the interaction picture gives

$$\tilde{H}_I(t) = e^{i(H_S+H_E)t} H_I e^{-i(H_S+H_E)t}. \quad (1.3)$$

If the coupling of the system and environment is taken as a closed quantum system, then the density operator in the interaction picture is

$$\tilde{\rho}(t) = |\tilde{\psi}(t)\rangle\langle\tilde{\psi}(t)|. \quad (1.4)$$

This equation encompasses ensembles of system states $\tilde{\psi}(t)$. Differentiating this density operator gives

$$\frac{\partial}{\partial t} \tilde{\rho}(t) = -i[\tilde{H}_I(t), \tilde{\rho}(t)] = \mathcal{L}(t)\tilde{\rho}(t), \quad (1.5)$$

which is classified as the form of the Liouville-von Neumann equation [7, 8]. The square brackets in this equation indicates the commutator between the Hamiltonian and the density operators transformed in the interaction picture and $\mathcal{L}(t)$ is the Liouville superoperator. The solution to Eq. (1.5) is

$$\tilde{\rho}(t) = \rho(0) - \imath \int_0^t ds [\tilde{H}_I(s), \tilde{\rho}(s)]. \quad (1.6)$$

By substituting this solution into Eq. (1.5) produces

$$\frac{\partial}{\partial t} \tilde{\rho}(t) = -\imath [\tilde{H}_I(t), \rho(0)] - \int_0^t ds [\tilde{H}_I(t), [\tilde{H}_I(s), \tilde{\rho}(s)]]. \quad (1.7)$$

By tracing over the environment degrees of freedom,

$$\frac{\partial}{\partial t} \text{tr}_E \tilde{\rho}(t) = -\text{tr}_E [\tilde{H}_I(t), \rho(0)] - \int_0^t ds \text{dstr}_E [\tilde{H}_I(t), [\tilde{H}_I(s), \tilde{\rho}(s)]]. \quad (1.8)$$

Substituting $\tilde{\rho}_S(t)$ in $\text{tr}_E \tilde{\rho}(t)$ given in Eq. (1.1) gives

$$\frac{\partial}{\partial t} \tilde{\rho}_S(t) = -\text{tr}_E [\tilde{H}_I(t), \rho(0)] - \int_0^t ds \text{dstr}_E [\tilde{H}_I(t), [\tilde{H}_I(s), \tilde{\rho}(s)]]. \quad (1.9)$$

Assuming that there is no correlations between S and E at the initial time $t = 0$, then the density operator is taken as

$$\rho(0) = \rho_S(0) \otimes \rho_E(0). \quad (1.10)$$

This assumption makes $\text{tr}_E [\tilde{H}_I(t), \rho(0)] = 0$, and therefore reduces Eq. (1.9) to

$$\frac{\partial}{\partial t} \tilde{\rho}_S(t) = - \int_0^t ds \text{dstr}_E [\tilde{H}_I(t), [\tilde{H}_I(s), \tilde{\rho}(s)]]. \quad (1.11)$$

We make use of the Born approximation, which suggests that: *the interaction is weak and the environment is sufficiently large so that the state of the environment is not affected by this coupling* [9]. The results of such an approximation indicates that the density operator of the environment remains unchanged throughout the evolution and the full density operator is

$$\tilde{\rho}(t) \approx \tilde{\rho}_S(t) \rho_E. \quad (1.12)$$

Substituting Eq. (1.12) in Eq. (1.11) gives

$$\frac{\partial}{\partial t} \tilde{\rho}_S(t) = - \int_0^t ds \text{dstr}_E [\tilde{H}_I(t), [\tilde{H}_I(s), \tilde{\rho}_S(s) \rho_E]]. \quad (1.13)$$

This shows that the future evolution of $\tilde{\rho}_S(t)$ depends on its past history through $\tilde{\rho}_S(s)$. The Markovian approximation elaborates that the environment memory time is extremely short compared to the system evolution [9]. Replacing $\tilde{\rho}_S(s) \rightarrow \tilde{\rho}_S(t)$ in Eq. (1.13) gives

$$\frac{\partial}{\partial t} \tilde{\rho}_S(t) = - \int_0^t dstr_E [\tilde{H}_I(t), [\tilde{H}_I(s), \tilde{\rho}_S(t) \rho_E]]. \quad (1.14)$$

This equation describes how the system $\rho_S(t)$ evolves under the system-environment interaction. For a specific system, we let the Hamiltonian in the interaction picture be defined as

$$\tilde{H}_I(t) = \sum_{\alpha} A_{\alpha}(t) \otimes B_{\alpha}(t). \quad (1.15)$$

Here A_{α} and B_{α} are system operators and environment operators respectively. The commutators in Eq. (1.14) can be expanded as follows,

$$\begin{aligned} \frac{\partial}{\partial t} \tilde{\rho}_S(t) &= - \int_0^t dstr_E [\tilde{H}_I(t), \tilde{H}_I(s) \tilde{\rho}_S(t) \rho_E - \tilde{\rho}_S(t) \rho_E \tilde{H}_I(s)] \\ &= - \int_0^t dstr_E \{ \tilde{H}_I(t) \tilde{H}_I(s) \tilde{\rho}_S(t) \rho_E - \tilde{H}_I(t) \tilde{\rho}_S(t) \rho_E \tilde{H}_I(s) \\ &\quad - \tilde{H}_I(s) \tilde{\rho}_S(t) \rho_E \tilde{H}_I(t) + \tilde{\rho}_S(t) \rho_E \tilde{H}_I(s) \tilde{H}_I(t) \}. \end{aligned} \quad (1.16)$$

The environment correlation function is taken as

$$C_{\alpha\beta}(t, s) = tr_E (B_{\alpha}(t) B_{\beta}(s) \rho_E). \quad (1.17)$$

Substituting Eq. (1.15) in Eq. (1.16) gives

$$\begin{aligned} \frac{\partial}{\partial t} \tilde{\rho}_S(t) &= - \int_0^t dstr_E \left\{ \left(\sum_{\alpha} A_{\alpha}(t) \otimes B_{\alpha}(t) \right) \left(\sum_{\beta} A_{\beta}(s) \otimes B_{\beta}(s) \right) \tilde{\rho}_S(t) \rho_E \right. \\ &\quad - \left(\sum_{\alpha} A_{\alpha}(t) \otimes B_{\alpha}(t) \right) \tilde{\rho}_S(t) \rho_E \left(\sum_{\beta} A_{\beta}(s) \otimes B_{\beta}(s) \right) \\ &\quad - \left(\sum_{\beta} A_{\beta}(s) \otimes B_{\beta}(s) \right) \tilde{\rho}_S(t) \rho_E \left(\sum_{\alpha} A_{\alpha}(t) \otimes B_{\alpha}(t) \right) \\ &\quad \left. + \tilde{\rho}_S(t) \rho_E \left(\sum_{\beta} A_{\beta}(s) \otimes B_{\beta}(s) \right) \left(\sum_{\alpha} A_{\alpha}(t) \otimes B_{\alpha}(t) \right) \right\}. \end{aligned} \quad (1.18)$$

This equation can be simplified as

$$\begin{aligned} \frac{\partial}{\partial t} \tilde{\rho}_S(t) = & - \sum_{\alpha\beta} \int_0^t dt ([A_\alpha(t), A_\beta(s) \tilde{\rho}_S(t)] C_{\alpha\beta}(t-s) \\ & + [\tilde{\rho}_S(t) A_\beta(s), A_\alpha(t)] C_{\beta\alpha}(s-t)). \end{aligned} \quad (1.19)$$

Transforming back to the Schrödinger picture gives

$$\begin{aligned} \frac{\partial}{\partial t} \rho_S(t) = & -i[H_S, \rho_S(t)] - \sum_{\alpha\beta} \int_0^t dt ([A_\alpha, A_\beta(s) \rho_S(t)] C_{\alpha\beta}(t-s) \\ & + [\rho_S(t) A_\beta(s), A_\alpha] C_{\beta\alpha}(s-t)). \end{aligned} \quad (1.20)$$

The first term on the right hand side of Eq. (1.20) describes the system evolution, and the remaining two terms describe the environmental influence on the system state. Eq. (1.20) derived above is said to be the Markovian master equation in Lindblad form.

The dynamics of a two level system coupled to the environment has been studied and is presented in this dissertation. However, this model is classified as non-Markovian due to strong system-environment coupling or initial states being correlated [10, 11, 12, 13]. This of-course disqualifies the Born and Markov approximations used to derive Eq. (1.20). Generalized or non-Markovian master equations [14, 15] are used instead to describe the dynamics of this model. In chapter 2 of the dissertation, the Generalized master equations are derived with the use of the Nakajima-Zwanzig technique [16, 17] and the time-convolutionless projection operator method. Stochastic wave-function methods are also used to treat the non-Markovian quantum master equations [18] numerically. The generalized Lindblad master equation is then unravelled for both strong and weak coupling regimes. In chapter 3 of the dissertation, the model is presented where both populations and coherences are derived. The Monte Carlo simulation is shown in chapter 4 where the jumps, realisations, and waiting times are found for both weak and strong coupling regimes. In chapter 5 is where the results are shown for both regimes. The MC simulations are compared with the time-convolutionless projection operator technique (TCL2).

Chapter 2

Generalized master equation and its Stochastic unravelling

2.1 Projection Operator Technique

In this part of the dissertation, a projection operator technique is presented to derive a non-Markovian master equations. This technique is based on the introduction of \mathcal{P} which acts on the total state of the system. The benefit of this technique is that it produces the mathematical expression that eliminates the degrees of freedom from the description of the states of the total system. The methodology followed in deriving these dynamical equations is adopted from reference [16, 17]. The starting point is to consider the projection superoperator \mathcal{P} acting on the states of the total system having the full density matrix ρ . The properties for the projection superoperator are,

$$\rho \rightarrow \mathcal{P}\rho \tag{2.1}$$

and

$$\mathcal{P}^2 = \mathcal{P}. \tag{2.2}$$

The projection $\mathcal{P}\rho$ represents an approximation of ρ which leads to a simplified effective description of the dynamics through a reduced set of variables. A reduced density matrix given in Eq. (1.1) is therefore written as

$$\rho_S(t) = \text{tr}_E \mathcal{P}\rho(t). \tag{2.3}$$

This is an equation of motion for $\mathcal{P}\rho$ which can either be the Nakajima-Zwanzig equation [16, 17], an integrodifferential equation with a retarded memory kernel, or the time-local differential equation of first order involving a time-dependent generator [18].

2.2 The Nakajima-Zwanzig projection operator technique

Let \mathcal{Q} and \mathcal{P} be two superoperators such that

$$\mathcal{Q}\rho = \rho - \mathcal{P}\rho \quad (2.4)$$

with the following properties

- $\mathcal{P} + \mathcal{Q} = I$
- $\mathcal{P}^2 = \mathcal{P}$
- $\mathcal{Q}^2 = \mathcal{Q}$
- $\mathcal{P}\mathcal{Q} = \mathcal{Q}\mathcal{P} = 0,$

where I represents the identity operator. Taking the partial derivative of $\mathcal{P}\rho$ gives

$$\frac{\partial}{\partial t}\mathcal{P}\rho(t) = \mathcal{P}\frac{\partial}{\partial t}\rho(t), \quad (2.5)$$

and using Eq. (1.5) results in

$$\frac{\partial}{\partial t}\mathcal{P}\rho(t) = \mathcal{P}\mathcal{L}(t)\rho(t). \quad (2.6)$$

Doing the same for the \mathcal{Q} superoperator gives

$$\frac{\partial}{\partial t}\mathcal{Q}\rho(t) = \mathcal{Q}\frac{\partial}{\partial t}\rho(t), \quad (2.7)$$

and

$$\frac{\partial}{\partial t}\mathcal{Q}\rho(t) = \mathcal{Q}\mathcal{L}(t)\rho(t). \quad (2.8)$$

The identity operator I is introduced in both Eqs. (2.6) and (2.8) as

$$\frac{\partial}{\partial t}\mathcal{P}\rho(t) = \mathcal{P}\mathcal{L}(t)[I]\rho(t) \quad (2.9)$$

and

$$\frac{\partial}{\partial t} \mathcal{Q}\rho(t) = \mathcal{Q}\mathcal{L}(t)[I]\rho(t). \quad (2.10)$$

Imposing the property $I = \mathcal{P} + \mathcal{Q}$ yields,

$$\frac{\partial}{\partial t} \mathcal{P}\rho(t) = \mathcal{P}\mathcal{L}(t)[\mathcal{P} + \mathcal{Q}]\rho(t) = \mathcal{P}\mathcal{L}(t)\mathcal{P}\rho(t) + \mathcal{P}\mathcal{L}(t)\mathcal{Q}\rho(t), \quad (2.11)$$

$$\frac{\partial}{\partial t} \mathcal{Q}\rho(t) = \mathcal{Q}\mathcal{L}(t)[\mathcal{P} + \mathcal{Q}]\rho(t) = \mathcal{Q}\mathcal{L}(t)\mathcal{P}\rho(t) + \mathcal{Q}\mathcal{L}(t)\mathcal{Q}\rho(t). \quad (2.12)$$

To solve for \mathcal{Q} in Eq. (2.12) requires integrating both sides of the equation

$$\int_{t_0}^t \left(\frac{\partial}{\partial t} \mathcal{Q}\rho(t) \right) ds = \int_{t_0}^t (\mathcal{Q}\mathcal{L}(t)\mathcal{P}\rho(t) + \mathcal{Q}\mathcal{L}(t)\mathcal{Q}\rho(t)) ds. \quad (2.13)$$

This gives,

$$\mathcal{Q}\rho(t) = \mathcal{G}(t, t_0)\mathcal{Q}\rho(t_0) + \int_{t_0}^t ds \mathcal{G}(t, s)\mathcal{Q}\mathcal{L}(s)\mathcal{P}\rho(s) \quad (2.14)$$

where the propagator $\mathcal{G}(t, s)$ is defined as

$$\mathcal{G}(t, s) \equiv T_{\leftarrow} \exp \left[\int_s^t ds' \mathcal{Q}\mathcal{L}(s') \right], \quad (2.15)$$

with T_{\leftarrow} describes the chronological time ordering from right to left. Substituting $\mathcal{Q}\rho(t)$ from Eq. (2.14) in Eq. (2.11) gives

$$\begin{aligned} \frac{\partial}{\partial t} \mathcal{P}\rho(t) &= \mathcal{P}\mathcal{L}(t)\mathcal{P}\rho(t) + \mathcal{P}\mathcal{L}(t)(\mathcal{G}(t, t_0)\mathcal{Q}\rho(t_0) \\ &\quad + \int_{t_0}^t ds \mathcal{P}\mathcal{L}(t)\mathcal{G}(t, s)\mathcal{Q}\mathcal{L}(s)\mathcal{P}\rho(s)). \end{aligned} \quad (2.16)$$

This equation is known as the Nakajima-Zwanzig equation. The degrees of freedom for this exact equation belong to the reduced system.

2.3 The time-convolutionless projection operator method

This technique expands the dynamics of the system of interest in terms of coupling strength by developing expressions for quantum master equation up to the fourth order in the coupling. It derives the exact master equation for the open system which is local in time. The time-convolutionless (TCL) projection operator technique eliminates the dependences

of the future time evolution on the history from the Nakajima-Zwanzig master equation defined in Eq. (2.16). If the density matrix $\rho(s)$ is introduced as

$$\rho(s) = G(t, s)(\mathcal{P} + \mathcal{Q})\rho(t) \quad (2.17)$$

where $G(t, s) = T_{\rightarrow}[-\int_s^t ds' \mathcal{L}(s')]$. The operator T_{\rightarrow} represents the chronological time ordering that increase from left to right. Taking this equation and substituting it in Eq. (2.14) gives

$$\mathcal{Q}\rho(t) = \mathcal{G}(t, t_0)\mathcal{Q}\rho(t_0) + \int_{t_0}^t ds \mathcal{G}(t, s)\mathcal{Q}\mathcal{L}(s)\mathcal{P}G(t, s)(\mathcal{P} + \mathcal{Q})\rho(t). \quad (2.18)$$

Now define the super-operator $\Sigma(t)$ as

$$\Sigma(t) = \int_{t_0}^t ds \mathcal{G}(t, s)\mathcal{Q}\mathcal{L}(s)\mathcal{P}G(t, s) \quad (2.19)$$

and substitute it in Eq. (2.18) gives

$$\mathcal{Q}\rho(t) = \mathcal{G}(t, t_0)\mathcal{Q}\rho(t_0) + \Sigma(t)\mathcal{P}\rho(t) + \Sigma(t)\mathcal{Q}\rho(t). \quad (2.20)$$

Solving for $\mathcal{Q}\rho(t)$ gives,

$$\mathcal{Q}\rho(t) = [1 - \Sigma(t)]^{-1}\Sigma(t)\mathcal{P}\rho(t) + [1 - \Sigma(t)]^{-1}\mathcal{G}(t, t_0)\mathcal{Q}\rho(t_0). \quad (2.21)$$

Inserting Eq. (2.21) in Eq. (2.11) gives

$$\begin{aligned} \frac{\partial}{\partial t}\mathcal{P}\rho(t) &= \mathcal{P}\mathcal{L}(t)\mathcal{P}\rho(t) + \mathcal{P}\mathcal{L}(t)[1 - \Sigma(t)]^{-1}\Sigma(t)\mathcal{P}\rho(t) \\ &\quad + \mathcal{P}\mathcal{L}(t)[1 - \Sigma(t)]^{-1}\mathcal{G}(t, t_0)\mathcal{Q}\rho(t_0). \end{aligned} \quad (2.22)$$

If the time-local generator is defined as

$$\mathcal{K}(t) = \mathcal{P}\mathcal{L}(t)[1 - \Sigma(t)]^{-1}\mathcal{P} \quad (2.23)$$

and the inhomogeneity is

$$\mathcal{I}(t) = \mathcal{P}\mathcal{L}(t)[1 - \Sigma(t)]^{-1}\mathcal{G}(t, t_0)\mathcal{Q}, \quad (2.24)$$

then Eq. (2.22) gives

$$\frac{d}{dt}\mathcal{P}\rho(t) = \mathcal{K}(t)\mathcal{P}\rho(t) + \mathcal{I}(t)\mathcal{Q}\rho(t_0). \quad (2.25)$$

This equation consists of exact and inhomogeneous terms namely generators $\mathcal{K}(t)$ and the $\mathcal{I}(t)$ which are time dependent. Expanding $[1 - \Sigma(t)]^{-1}$ into a geometric series gives

$$[1 - \Sigma(t)]^{-1} = \sum_{n=0}^{\infty} [\Sigma(t)]^n. \quad (2.26)$$

Substituting Eq. (2.26) into Eq. (2.23) gives

$$\mathcal{K}(t) = \mathcal{P}\mathcal{L}(t) \sum_{n=0}^{\infty} [\Sigma(t)]^n \mathcal{P}, \quad (2.27)$$

and this expression can be written as

$$\mathcal{K}(t) = \sum_{n=1}^{\infty} \mathcal{K}_n(t). \quad (2.28)$$

Re-writing the super-operator $\Sigma(t)$ as

$$\Sigma(t) = \sum_{n=1}^{\infty} \Sigma_n(t), \quad (2.29)$$

and introducing it in Eq. (2.28) gives

$$\mathcal{K}(t) = \sum_{n=1}^{\infty} \mathcal{K}_n(t) = \mathcal{P}\mathcal{L}(t) \sum_{n=0}^{\infty} [\Sigma_n(t)]^n \mathcal{P}. \quad (2.30)$$

Eq. (2.30) represents the TCL generator ($\mathcal{K}(t)$) that is time-dependent. The full system dynamics of a non-Markovian process is governed by Eq. (2.30). The solution of Eq. (2.30) is determined by a perturbation expansion with n representing the order of the TCL expansion.

2.4 Structure of non-Markovian master equation

The time-convolutionless projection operator technique gives the dynamical equation of the density matrix. Following the assumption that $\mathcal{Q}\rho(t_0) = 0$, then Eq. (2.25) is

$$\frac{d}{dt} \mathcal{P}\rho(t) = \mathcal{K}^t(\mathcal{P}\rho(t)). \quad (2.31)$$

The operator \mathcal{K}^t is a linear generator that depends on time. Applying Eq. (2.1) to Eq. (2.31) gives the system of equations of motion for the densities as

$$\frac{d}{dt} \rho_i = \mathcal{K}_i^t(\rho_1, \dots, \rho_n), \quad (2.32)$$

where $i = 1, 2, 3, \dots, n$. The linear generators in this form may be approximated by time-independent generators as

$$\frac{d}{dt}\rho_i = \mathcal{K}_i(\rho_1, \dots, \rho_n). \quad (2.33)$$

This equation is assumed to preserve the positivity of all components ρ_i . Dynamical transformation is formulated by introducing an auxiliary Hilbert space C^m and an orthonormal basis $|i\rangle$ for this space. The vector ϱ density matrix on the extended space $\mathcal{H}_S \otimes C^m$ is

$$\varrho = \sum_i \rho_i \otimes |i\rangle\langle i|. \quad (2.34)$$

Taking the partial trace of ϱ over the auxiliary space gives the reduced density matrix ρ_S . The auxiliary space represents an additional degrees of freedom which express the statistical correlations. Employing the fact that there exists a Lindblad generator \mathcal{L} on this space ensures the conservation of the positivity condition. The mathematical presentation of this condition can be expressed as

$$\mathcal{L}\left(\sum_i \rho_i \otimes |i\rangle\langle i|\right) = \sum_i \mathcal{K}_i(\rho_1, \dots, \rho_n) \otimes |i\rangle\langle i|, \quad (2.35)$$

with solution

$$\sum_i \rho_i(t) \otimes |i\rangle\langle i| = e^{\mathcal{L}t} \left(\sum_i \rho_i(0) \otimes |i\rangle\langle i| \right). \quad (2.36)$$

Using the theorem from reference [10] which states as follows.

Theorem: A Lindblad generator \mathcal{L} on the extended state space with property mentioned at Eq. (2.35) exists if and only if the generators \mathcal{K}_i can be represented as

$$\mathcal{K}_i(\rho_1, \dots, \rho_n) = -i[H^i, \rho_i] + \sum_{j\lambda} (R_\lambda^{ij} \rho_j R_\lambda^{ij\dagger} - \frac{1}{2} \{R_\lambda^{ji\dagger} R_\lambda^{ji}, \rho_i\}). \quad (2.37)$$

The operators H^i and R_λ^{ij} represent Hermitian operators and arbitrary system operator respectively. Substituting Eq. (2.37) into Eq. (2.33) gives the master equation as

$$\frac{d}{dt}\rho_i = -i[H^i, \rho_i] + \sum_{j\lambda} (R_\lambda^{ij} \rho_j R_\lambda^{ij\dagger} - \frac{1}{2} \{R_\lambda^{ji\dagger} R_\lambda^{ji}, \rho_i\}). \quad (2.38)$$

Eq. (2.38) is the general form for equations of motion of dynamical variables ρ_i . The indices i and j are summed over $1, 2, \dots, n$. It should be noted that if $R_\lambda^{ij} = \delta_{ij} R_\lambda^i$, then Eq. (2.38) reduces to a master equation for the reduced density matrix in Lindblad form.

2.5 Unravelling the quantum master equation

An unravelling approach is when a stochastic equation of motion for the reduced state vector involves a multiple time integration over the system history. With this method it is possible to construct an exact stochastic Schrödinger equation which describes the non-Markovian time evolution of an open quantum system. It is performed by taking n random state vectors $|\psi_i(t)\rangle$ that satisfy the stochastic differential equation for a piecewise deterministic process (PDP) in Hilbert space [1]. The piecewise deterministic process is simply defined as a stochastic process that is obtained by combining a deterministic time-evolution with a jump process [4]. The strategy followed in unravelling Eq. (2.38) is adopted from reference [4]. The starting point is to describe the state of the open system by a pair of stochastic wave functions as

$$|\psi_i\rangle = \begin{pmatrix} |\psi_1\rangle \\ |\psi_2\rangle \end{pmatrix}. \quad (2.39)$$

The wave function $|\psi_i\rangle$ becomes a stochastic process in Hilbert space with probability functional $P[|\psi_i\rangle, t]$ defined as

$$P[|\psi_i\rangle, t] = \int D|\psi_j\rangle D\langle\psi_j| T[|\psi_i\rangle, t | |\psi_j\rangle, t_0] P[|\psi_j\rangle, t_0]. \quad (2.40)$$

Here $T[|\psi_i\rangle, t | |\psi_j\rangle, t_0]$ is the conditional transition probability of the process and $D|\psi_j\rangle D\langle\psi_j|$ represents the volume element. The mathematical representation of the volume element is taken as

$$D|\psi_j\rangle D\langle\psi_j| = \prod_j \frac{1}{2} d|\psi_j\rangle d\langle\psi_j|. \quad (2.41)$$

The density operators are then given by the expectation values as

$$\rho_i(t) = E(|\psi_i(t)\rangle\langle\psi_i(t)|) = \int D|\psi_i\rangle D\langle\psi_i| P[|\psi_i\rangle, t] |\psi_i(t)\rangle\langle\psi_i(t)|. \quad (2.42)$$

The wave functions $\langle\psi_i|\psi_i\rangle$ are bounded between 0 and 1, and

$$\sum_i \langle\psi_i(t)|\psi_i(t)\rangle \equiv 1, \quad (2.43)$$

which implies that the reduced density matrix can then be expressed as

$$\rho_S(t) = \sum_i \rho_i(t). \quad (2.44)$$

The stochastic differential equation for the process $|\psi_i\rangle$ is

$$d|\psi_i\rangle = -iG_i|\psi_i\rangle dt + \sum_{j\lambda} \left[\frac{R_\lambda^{ij}|\psi_j\rangle}{\|R_\lambda^{ij}|\psi_j\rangle\|} - |\psi_i\rangle \right] dN_\lambda^j(t), \quad (2.45)$$

where $dN_\lambda^j(t)$ represents the Poisson increments [4]. The conditions for the Poisson increments are

$$E[dN_\lambda^j(t)] = \frac{\sum_{j\lambda} \|R_\lambda^{ij}(t)|\psi_i(t)\|^2}{\sum_i \|\psi_i(t)\|^2} dt, \quad (2.46)$$

$$dN_\lambda^j(t)dN_\lambda^k(t) = \delta_{ji}dN_\lambda^j(t). \quad (2.47)$$

The non-linear operator $G_i|\psi_i\rangle$ which describe the deterministic drift is defined as

$$G_i|\psi_i\rangle = H^i - \frac{i}{2} \sum_{j\lambda} (R_\lambda^{ji\dagger} R_\lambda^{ji} - \|R_\lambda^{ij}|\psi_j\rangle\|^2). \quad (2.48)$$

The first term in Eq. (2.45) represents the generator corresponding to the deterministic time-evolution equation

$$\frac{d}{dt}|\psi_i\rangle = -iG_i|\psi_i\rangle. \quad (2.49)$$

The second term represents the possible jumps for the upper and lower bands of the system. They are written as

$$|\psi_i\rangle \rightarrow \frac{R_\lambda^{ij}|\psi_j\rangle}{\|R_\lambda^{ij}|\psi_j\rangle\|}. \quad (2.50)$$

The rate at which the jump takes is

$$M_\lambda^j = \sum_i \|R_\lambda^{ij}|\psi_j\rangle\|^2. \quad (2.51)$$

The realisations of the jumps are defined as

$$|\psi_i\rangle \rightarrow \frac{e^{-iG_i t}|\psi_j\rangle}{\|e^{-iG_i t}|\psi_j\rangle\|}. \quad (2.52)$$

The Eqs. (2.50), (2.51), and (2.52) are deduced from Eq. (2.45) to enlight the jump processes between a lower and upper bands. The total waiting time distribution which is a quantity that defines the probability for the next jump to occur is

$$F(\tau) = 1 - \exp \left[- \sum_{ij,\lambda} \|R_\lambda^{ij}|\psi_j\rangle\|^2 \tau \right], \quad (2.53)$$

where τ represents the waiting time before the jump. It should be noted that Eq. (2.42) obeys Eq. (2.38) which provides unravelling of Eq. (2.45). In the next chapter, we introduce the model studied in terms of its Hamiltonian, and apply a technique of TCL expansion using the correlated projection superoperator. This technique will be able to provide the equations of motion for the two level system coupled with an environment. The solutions of the equations of motions will provide us with the populations and the coherences.

Chapter 3

Model and Time Convolutionless Approximation

3.1 Two level system

A two-level system S coupled to an environment E shown in Fig. (3.1) has been studied.

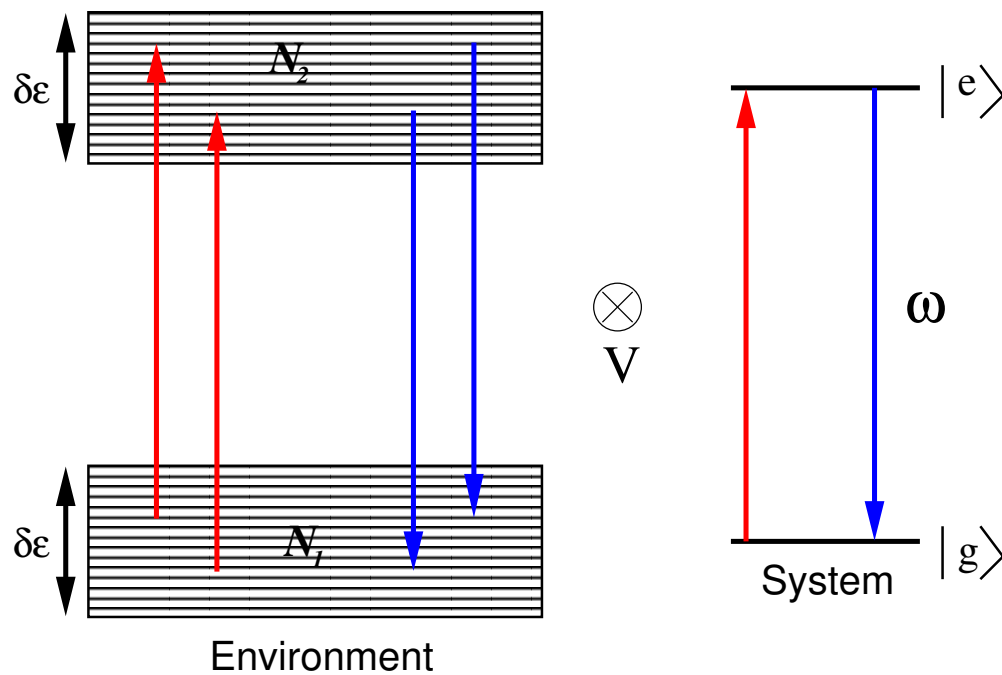


Figure 3.1: Two level system coupled to the environment [2].

The level spacing ω separates the excited $|e\rangle = |1\rangle$ and ground $|g\rangle = |0\rangle$ states of the system. This system is coupled to an environment consisting of the number of energy levels N_1 and N_2 , and the width of the bands $\delta\epsilon$ with the interaction potential V . The Hamiltonian for this model can be separated into two parts $H = H_0 + V$ where

$$H_0 = \omega\sigma_z + \sum_{n_1} \frac{\delta\epsilon}{N_1} n_1 |n_1\rangle\langle n_1| + \sum_{n_2} \left(\omega + \frac{\delta\epsilon}{N_2} n_2\right) |n_2\rangle\langle n_2|, \quad (3.1)$$

and

$$V = \lambda \sum_{n_1, n_2} c(n_1, n_2) \sigma_+ |n_1\rangle\langle n_2| + H.c. \quad (3.2)$$

The basis $|n_1\rangle$ and $|n_2\rangle$ denote the lower and upper bands respectively. σ_z is the Pauli matrix, $\sigma_+ = \sigma_x + i\sigma_y$, and λ represents the strength of the interaction. The independent coupling constants $c(n_1, n_2)$ are complex Gaussian random variables with zero mean and unit variance. In the following section equations of motion are derived for the two level system coupled to an environment.

3.2 TCL expansion using the correlated projection superoperator

By considering a two level system coupled to an environment as the model of interest, one uses the fact that the dynamics of the composite system are governed by the Hamiltonian $H = H_0 + V$. Interaction representation of the Hamiltonian defined above is used to derive equations of motion in this approach. We have followed what reference [11] has published in deriving equations of motion. If one denotes the projections Π_1 and Π_2 onto the lower and upper bands as

$$\Pi_1 = \sum_{n_1} |n_1\rangle\langle n_1|, \quad (3.3)$$

and

$$\Pi_2 = \sum_{n_2} |n_2\rangle\langle n_2|. \quad (3.4)$$

These projections satisfy the following conditions

$$\Pi_i \Pi_j = \delta_{ij}$$

and

$$\sum_i \Pi_i = I$$

which are the requirements for the projection operator. Here indexes $i = 1$ and $j = 2$, I is the identity matrix, and $\delta\epsilon_{ij}$ represent the trace over the environment. We use these projections in the projection superoperator that is acting on the density operator is

$$\begin{aligned} \mathcal{P}\rho &= tr_E\{\Pi_1\rho\} \otimes \frac{1}{N_1}\Pi_1 + tr_E\{\Pi_2\rho\} \otimes \frac{1}{N_2}\Pi_2 \\ &= \rho_S^{(1)} \otimes \frac{1}{N_1}\Pi_1 + \rho_S^{(2)} \otimes \frac{1}{N_2}\Pi_2. \end{aligned} \quad (3.5)$$

The density matrices $\rho_S^{(1)}$ and $\rho_S^{(2)}$ characterize the dynamical variables which are correlated with the projections onto the lower and upper bands. The total reduced system state is then defined as

$$\rho_S(t) = tr_E\{\mathcal{P}\rho(t)\} = \rho_S^{(1)}(t) + \rho_S^{(2)}(t). \quad (3.6)$$

The initial state of the correlated form is taken to be

$$\rho(0) = \rho_S^{(1)}(0) \otimes \frac{1}{N_1}\Pi_1 + \rho_S^{(2)}(0) \otimes \frac{1}{N_2}\Pi_2. \quad (3.7)$$

Taking the derivative of Eq. (3.5) with respect to time lead to

$$\frac{d}{dt}\mathcal{P}\rho(t) = \dot{\rho}_S^{(1)}(t) \otimes \frac{1}{N_1}\Pi_1 + \dot{\rho}_S^{(2)}(t) \otimes \frac{1}{N_2}\Pi_2. \quad (3.8)$$

From Eq. (2.30), the second-order contribution of TCL generator is

$$\mathcal{K}_2(t) = \int_0^t dt_1 \mathcal{P}\mathcal{L}(t)\mathcal{L}(t_1)\mathcal{P}. \quad (3.9)$$

Applying Eq. (3.8) in Eq. (2.25) with the absence of the second term since $\mathcal{Q}\rho(t_0)$ is assumed to be zero, and introducing the two level system will give

$$\begin{aligned} \mathcal{K}_2(t)\mathcal{P}\rho(t) &= \int_0^t dt_1 h(t-t_1) [2\gamma_1\sigma_+\rho_S^{(2)}\sigma_- \\ &- \gamma_2\{\sigma_+\sigma_-, \rho_S^{(1)}\}] \otimes \frac{1}{N_1}\Pi_1 + \int_0^t dt_1 h(t-t_1) \\ &\times [2\gamma_2\sigma_-\rho_S^{(1)}\sigma_+ - \gamma_1\{\sigma_-\sigma_+, \rho_S^{(2)}\}] \otimes \frac{1}{N_2}\Pi_2. \end{aligned} \quad (3.10)$$

The function $h(t-t_1)$ is

$$h(t) = \frac{\delta\epsilon}{2\pi} \frac{\sin^2(\delta\epsilon t/2)}{(\delta\epsilon t/2)^2}, \quad (3.11)$$

and it called a two-point environment correlation function. The relaxation rates γ_1 and γ_2 are defined as

$$\gamma_{1,2} = \frac{2\pi\lambda^2 N_{1,2}}{\delta\epsilon}. \quad (3.12)$$

The interaction is weak if a Markovian condition which says $\gamma_{1,2} \ll \delta\epsilon$ and the condition which says $\delta\epsilon t \gg 1$ are satisfied [10]. With that Eq. (3.10) becomes

$$\begin{aligned} \mathcal{K}_2(t)\mathcal{P}\rho(t) &= \int_0^t dt_1 \frac{1}{2} [2\gamma_1 \sigma_+ \rho_S^{(2)} \sigma_- \\ &- \gamma_2 \{\sigma_+ \sigma_-, \rho_S^{(1)}\}] \otimes \frac{1}{N_1} \Pi_1 + \int_0^t dt_1 h(t-t_1) \\ &\times [2\gamma_2 \sigma_- \rho_S^{(1)} \sigma_+ - \gamma_1 \{\sigma_- \sigma_+, \rho_S^{(2)}\}] \otimes \frac{1}{N_2} \Pi_2. \end{aligned} \quad (3.13)$$

Relating the terms in Eq. (3.8) with terms in Eq. (3.13) the equations of motion are:

$$\frac{d}{dt} \rho_S^{(1)}(t) = \gamma_1 \sigma_+ \rho_S^{(2)} \sigma_- - \frac{\gamma_2}{2} \{\sigma_+ \sigma_-, \rho_S^{(1)}\}, \quad (3.14)$$

and

$$\frac{d}{dt} \rho_S^{(2)}(t) = \gamma_2 \sigma_- \rho_S^{(1)} \sigma_+ - \frac{\gamma_1}{2} \{\sigma_- \sigma_+, \rho_S^{(2)}\}. \quad (3.15)$$

When both bands are initially populated, i.e. $\rho_S^{(1)}(0)$ and $\rho_S^{(2)}(0)$ are not equal to zero, then the solutions for the lower and upper bands of the system [2] are:

$$\begin{aligned} \rho_{11} &= \rho_{11}(0) \left[\frac{\gamma_1}{\gamma_1 + \gamma_2} + \frac{\gamma_2}{\gamma_1 + \gamma_2} e^{-(\gamma_1 + \gamma_2)t} \right] \\ &+ \rho_{22}(0) \left[\frac{\gamma_1}{\gamma_1 + \gamma_2} - \frac{\gamma_1}{\gamma_1 + \gamma_2} e^{-(\gamma_1 + \gamma_2)t} \right], \end{aligned} \quad (3.16)$$

and

$$\begin{aligned} \rho_{22} &= \rho_{22}(0) \left[\frac{\gamma_2}{\gamma_1 + \gamma_2} + \frac{\gamma_1}{\gamma_1 + \gamma_2} e^{-(\gamma_1 + \gamma_2)t} \right] \\ &+ \rho_{11}(0) \left[\frac{\gamma_2}{\gamma_1 + \gamma_2} - \frac{\gamma_2}{\gamma_1 + \gamma_2} e^{-(\gamma_1 + \gamma_2)t} \right]. \end{aligned} \quad (3.17)$$

The coherences which are both off-diagonal terms of the reduced density matrix are found to be,

$$\rho_{12} = \rho_{12}(0) \left[\frac{\gamma_1}{\gamma_1 + \gamma_2} + \frac{\gamma_2}{\gamma_1 + \gamma_2} e^{-(\gamma_1 + \gamma_2)t} \right] \quad (3.18)$$

and

$$\rho_{21} = \rho_{21}(0) \left[\frac{\gamma_2}{\gamma_1 + \gamma_2} + \frac{\gamma_1}{\gamma_1 + \gamma_2} e^{-(\gamma_1 + \gamma_2)t} \right]. \quad (3.19)$$

For the strong coupling, when $\delta\epsilon t \gg 1$ does not hold, then the equations of motion are

$$\frac{d}{dt}\rho_S^{(1)}(t) = \int_0^t dt_1 h(t-t_1)[2\gamma_1\sigma_+\rho_S^{(2)}(t)\sigma_- - \gamma_2\{\sigma_+\sigma_-, \rho_S^1(t)\}], \quad (3.20)$$

and

$$\frac{d}{dt}\rho_S^{(2)}(t) = \int_0^t dt_1 h(t-t_1)[2\gamma_2\sigma_-\rho_S^{(1)}(t)\sigma_+ - \gamma_1\{\sigma_-\sigma_+, \rho_S^2(t)\}]. \quad (3.21)$$

The solutions for the lower and upper bands of the system are:

$$\rho_{11} = \rho_{11}(0) \left[\frac{\gamma_1}{\gamma_1 + \gamma_2} + \frac{\gamma_2}{\gamma_1 + \gamma_2} e^{-\Gamma(t)} \right] + \rho_{22}(0) \left[\frac{\gamma_1}{\gamma_1 + \gamma_2} - \frac{\gamma_1}{\gamma_1 + \gamma_2} e^{-\Gamma(t)} \right], \quad (3.22)$$

and

$$\rho_{22} = \rho_{22}(0) \left[\frac{\gamma_1}{\gamma_1 + \gamma_2} - \frac{\gamma_1}{\gamma_1 + \gamma_2} e^{-\Gamma(t)} \right] + \rho_{11}(0) \left[\frac{\gamma_2}{\gamma_1 + \gamma_2} - \frac{\gamma_2}{\gamma_1 + \gamma_2} e^{-\Gamma(t)} \right]. \quad (3.23)$$

The coherences are

$$\rho_{12} = \rho_{12}(0) \left[\frac{\gamma_1}{\gamma_1 + \gamma_2} + \frac{\gamma_2}{\gamma_1 + \gamma_2} e^{-\Gamma(t)} \right] \quad (3.24)$$

and

$$\rho_{21} = \rho_{21}(0) \left[\frac{\gamma_1}{\gamma_1 + \gamma_2} + \frac{\gamma_2}{\gamma_1 + \gamma_2} e^{-\Gamma(t)} \right]. \quad (3.25)$$

Here $\Gamma(t)$ is

$$\Gamma(t) = 2(\gamma_1 + \gamma_2) \int_0^t dt_1 \int_0^{t_1} dt_2 h(t_1 - t_2). \quad (3.26)$$

It is clear that the solutions of the equations of motion for both weak and strong couplings highly depend on the relaxation rates. For the weak coupling, the populations and the coherences depend on the time-independent rate $(\gamma_{1,2})$. For the strong coupling, the populations and the coherences depend on both the time-independent rate $(\gamma_{1,2})$ and the time-dependent rate $(\Gamma(t))$ where a Gaussian quadrature algorithm was used to evaluate the integral of $h(t_1 - t_2)$. The relaxation rates $\gamma_{1,2}$ defined in Eq. (3.12) contain the environment energy levels $N_{1,2}$, coupling strength λ , and energy band width $\delta\epsilon$. For the model studied in this dissertation, $\lambda = 0.001$ was taken to be in the weak coupling regime to satisfy the Markovian condition. For the strong coupling regime $\lambda = 0.01$ chosen. These were kept constant throughout the simulation of our system. The environment energy levels $N_{1,2}$ and energy band width $\delta\epsilon$ were varied interchangeably.

Chapter 4

Stochastic wave-function simulations

4.1 Monte Carlo simulations

The following analysis gives details of the Monte Carlo wave-function simulation for the two level system coupled with an environment. The starting point is to consider our density matrix defined in Eq. (2.38), in this equation we let $i = 1$ and $j = 2$. The operators are then transformed into superscripts 1 and 2 namely H^1 , H^2 , R^{11} , R^{12} , and R^{22} . We then let

$$\begin{aligned} H^1 &= H^2 = 0, \\ R^{11} &= R^{22} = 0, \\ R^{12} &= \sqrt{\gamma_1}\sigma_+, \\ R^{21} &= \sqrt{\gamma_2}\sigma_-. \end{aligned} \tag{4.1}$$

It should be noted that if these conditions are substituted in Eq. (2.38), then Eqs. (3.14), (3.15), (3.20), and (3.21) can be obtained both for strong and weak couplings regimes. If one substitutes Eq. (4.1) in Eq. (2.48), then

$$\begin{aligned} G_1 &= H^1 - \frac{i}{2}(R^{12\dagger}R^{12} - \|R^{21}|\psi_1\rangle I\|^2 - \|R^{12}|\psi_2\rangle I\|^2) \\ &= -\frac{i}{2}(\gamma_1\sigma_+\sigma_- - \gamma_2c_1I - \gamma_1c_2I), \end{aligned} \tag{4.2}$$

Here $c_1 = \|\sigma_-|\psi_1\rangle\|^2$ and $c_2 = \|\sigma_+|\psi_2\rangle\|^2$. By substituting the matrix terms $\sigma_+ = \begin{pmatrix} 0 & 1 \\ 0 & 0 \end{pmatrix}$, $\sigma_- = \begin{pmatrix} 0 & 0 \\ 1 & 0 \end{pmatrix}$, and $I = \begin{pmatrix} 1 & 0 \\ 0 & 1 \end{pmatrix}$, we have

$$\begin{aligned}
G_1 &= -\frac{\imath}{2} \left[\gamma_1 \begin{pmatrix} 0 & 1 \\ 0 & 0 \end{pmatrix} \begin{pmatrix} 0 & 0 \\ 1 & 0 \end{pmatrix} - \gamma_2 c_1 \begin{pmatrix} 1 & 0 \\ 0 & 1 \end{pmatrix} - \gamma_1 c_2 \begin{pmatrix} 1 & 0 \\ 0 & 1 \end{pmatrix} \right] \\
&= -\frac{\imath}{2} \left[\begin{pmatrix} \gamma_1 & 0 \\ 0 & 0 \end{pmatrix} - \begin{pmatrix} \gamma_2 c_1 & 0 \\ 0 & \gamma_2 c_1 \end{pmatrix} - \begin{pmatrix} \gamma_1 c_2 & 0 \\ 0 & \gamma_1 c_2 \end{pmatrix} \right] \\
&= -\frac{\imath}{2} \begin{pmatrix} \gamma_1 - \gamma_2 c_1 - \gamma_1 c_2 & 0 \\ 0 & -\gamma_1 c_2 - \gamma_2 c_1 \end{pmatrix}. \tag{4.3}
\end{aligned}$$

Similarly for G_2 we have

$$\begin{aligned}
G_2 &= H^1 - \frac{\imath}{2} (R^{21\dagger} R^{21} - \|R^{21}|\psi_1\rangle I\|^2 - \|R^{12}|\psi_2\rangle I\|^2) \\
&= -\frac{\imath}{2} (\gamma_2 \sigma_- \sigma_+ - \gamma_2 c_1 I - \gamma_1 c_2 I) \\
&= -\frac{\imath}{2} \left[\gamma_2 \begin{pmatrix} 0 & 0 \\ 1 & 0 \end{pmatrix} \begin{pmatrix} 0 & 1 \\ 0 & 0 \end{pmatrix} - \gamma_2 c_1 \begin{pmatrix} 1 & 0 \\ 0 & 1 \end{pmatrix} - \gamma_1 c_2 \begin{pmatrix} 1 & 0 \\ 0 & 1 \end{pmatrix} \right] \\
&= -\frac{\imath}{2} \left[\begin{pmatrix} 0 & 0 \\ 0 & \gamma_1 \end{pmatrix} - \begin{pmatrix} \gamma_2 c_1 & 0 \\ 0 & \gamma_2 c_1 \end{pmatrix} - \begin{pmatrix} \gamma_1 c_2 & 0 \\ 0 & \gamma_1 c_2 \end{pmatrix} \right] \\
&= \frac{\imath}{2} \begin{pmatrix} -\gamma_2 c_1 - \gamma_1 c_2 & 0 \\ 0 & \gamma_1 - \gamma_2 c_1 - \gamma_1 c_2 \end{pmatrix}. \tag{4.4}
\end{aligned}$$

Eqs. (4.3) and (4.4) represent the drift terms (G_1 and G_2) for the two state vectors $|\psi_1\rangle$ and $|\psi_2\rangle$. . If again Eq. (4.1) is substituted in Eq. (2.50), then one gets the two possible jumps as:

$$|\psi_1\rangle \rightarrow 0, |\psi_2\rangle \rightarrow \frac{\sigma_-|\psi_1\rangle}{\|\sigma_-|\psi_1\rangle\|}, \tag{4.5}$$

with jump rate defined in Eq. (2.51) as $M^1 = \gamma_2 \|\sigma_-|\psi_1\rangle\|^2$ and

$$|\psi_1\rangle \rightarrow \frac{\sigma_+|\psi_2\rangle}{\|\sigma_+|\psi_2\rangle\|}, |\psi_2\rangle \rightarrow 0 \tag{4.6}$$

with jump rate defined in Eq. (2.51) $M^2 = \gamma_2 \|\sigma_+ |\psi_2\rangle\|^2$. Without loss of generality, let the state vector $|\psi_1\rangle = \begin{pmatrix} a_1 \\ b_1 \end{pmatrix}$, and substituting it in Eq. (4.5) gives,

$$|\psi_1\rangle \rightarrow 0, |\psi_2\rangle = \begin{pmatrix} 0 \\ 1 \end{pmatrix}, \quad (4.7)$$

the jump rate is $M^1 = \gamma_2 \|\sigma_- |\psi_1\rangle\|^2 = \gamma_2 a_1$. Similarly for the state vector $|\psi_2\rangle = \begin{pmatrix} a_2 \\ b_2 \end{pmatrix}$, and substituting it in Eq. (4.6) gives, $M^2 = \gamma_1 \|\sigma_+ |\psi_2\rangle\|^2 = \gamma_1 b_1$. The realisation defined in Eq. (2.52) for the state vector $|\psi_1\rangle$ is

$$|\tilde{\psi}_1(t)\rangle \rightarrow \frac{e^{-iG_1 t} |\psi_1\rangle}{\|e^{-iG_1 t} |\psi_1\rangle\|}, \quad (4.8)$$

and can be represented in terms of $|\psi_1\rangle = \begin{pmatrix} a_1 \\ b_1 \end{pmatrix}$ and by Eq. (4.3) as follows:

The numerator of Eq. 4.8 is

$$\begin{aligned} e^{-iG_1 t} |\psi_1\rangle &= \begin{pmatrix} e^{-\frac{1}{2}(\gamma_1 - \gamma_2 c_1 - \gamma_1 c_1)t} & 0 \\ 0 & e^{-\frac{1}{2}(-\gamma_2 c_1 - \gamma_1 c_2)t} \end{pmatrix} \begin{pmatrix} a_1 \\ b_1 \end{pmatrix} \\ &= \begin{pmatrix} a_1 e^{-\frac{1}{2}(\gamma_1 - \gamma_2 c_1 - \gamma_1 c_1)t} \\ b_1 e^{-\frac{1}{2}(-\gamma_2 c_1 - \gamma_1 c_2)t} \end{pmatrix}. \end{aligned} \quad (4.9)$$

The denominator of Eq. (4.8) is

$$\begin{aligned} \|e^{iG_1 t} |\psi_1\rangle\|^2 &= \left\| \begin{pmatrix} a_1 e^{-\frac{1}{2}(\gamma_1 - \gamma_2 c_1 - \gamma_1 c_1)t} \\ b_1 e^{-\frac{1}{2}(-\gamma_2 c_1 - \gamma_1 c_2)t} \end{pmatrix} \right\|^2 \\ &= \begin{pmatrix} a_1 e^{-\frac{1}{2}(\gamma_1 - \gamma_2 c_1 - \gamma_1 c_1)t} \\ b_1 e^{-\frac{1}{2}(-\gamma_2 c_1 - \gamma_1 c_2)t} \end{pmatrix} \begin{pmatrix} a_1 e^{-\frac{1}{2}(\gamma_2 - \gamma_2 c_1 - \gamma_1 c_2)t} & b_1 e^{-\frac{1}{2}(-\gamma_2 c_1 - \gamma_1 c_2)t} \end{pmatrix} \\ &= a_1^2 e^{(-\gamma_1 + \gamma_2 c_1 + \gamma_1 c_2)t} + b_1^2 e^{(\gamma_2 c_1 + \gamma_1 c_2)t}. \end{aligned} \quad (4.10)$$

Putting Eqs. (4.9) and (4.10) back to Eq. (4.8) gives,

$$|\tilde{\psi}_1(t)\rangle = \begin{pmatrix} 1 \\ 0 \end{pmatrix}. \quad (4.11)$$

The realisation for the state vector $|\psi_2\rangle$ is

$$|\tilde{\psi}_2(t)\rangle \rightarrow \frac{e^{-iG_2t}|\psi_2\rangle}{\|e^{-iG_2(t)}|\psi_2\rangle\|}, \quad (4.12)$$

and can be represented in terms of $|\psi_1\rangle = \begin{pmatrix} a_2 \\ b_2 \end{pmatrix}$ and Eq. (4.4) as follows:

The numerator of Eq. (4.12) is

$$\begin{aligned} e^{iG_2t}|\psi_2\rangle &= \begin{pmatrix} e^{-\frac{1}{2}(\gamma_2-\gamma_2c_1-\gamma_1c_2)t} & 0 \\ 0 & e^{-\frac{1}{2}(-\gamma_2c_1-\gamma_1c_2)t} \end{pmatrix} \begin{pmatrix} a_2 \\ b_2 \end{pmatrix} \\ &= \begin{pmatrix} a_2e^{-\frac{1}{2}(\gamma_2-\gamma_2c_1-\gamma_1c_2)t} \\ b_2e^{-\frac{1}{2}(-\gamma_2c_1-\gamma_1c_2)t} \end{pmatrix} \end{aligned} \quad (4.13)$$

The denominator of Eq. (4.12) is

$$\begin{aligned} \|e^{iG_2t}|\psi_2\rangle\| &= \left\| \begin{pmatrix} a_2e^{-\frac{1}{2}(\gamma_2-\gamma_2c_1-\gamma_1c_2)t} \\ b_2e^{-\frac{1}{2}(-\gamma_2c_1-\gamma_1c_2)t} \end{pmatrix} \right\| \\ &= \begin{pmatrix} a_2e^{-\frac{1}{2}(\gamma_2-\gamma_2c_1-\gamma_1c_2)t} \\ b_2e^{-\frac{1}{2}(-\gamma_2c_1-\gamma_1c_2)t} \end{pmatrix} \begin{pmatrix} a_2e^{-\frac{1}{2}(\gamma_2-\gamma_2c_1-\gamma_1c_2)t} & b_2e^{-\frac{1}{2}(-\gamma_2c_1-\gamma_1c_2)t} \end{pmatrix} \\ &= (a_2^2e^{-(\gamma_2-\gamma_2c_1-\gamma_1c_1)t} + b_2^2e^{-(\gamma_2c_1-\gamma_1c_2)t})^{\frac{1}{2}}. \end{aligned} \quad (4.14)$$

Putting Eqs. (4.13) and (4.10) back to Eq. (4.12) gives,

$$|\tilde{\psi}_2(t)\rangle = \begin{pmatrix} 0 \\ 1 \end{pmatrix}. \quad (4.15)$$

Eqs.(4.11) and (4.15) represent the realisations for the state vectors $|\psi_1\rangle$ and $|\psi_2\rangle$. The total waiting time distribution defined in Eq. (2.53) for the weak coupling regime is

$$\begin{aligned} F(\tau) &= 1 - \exp[-\gamma_1\|\sigma_+|\psi_2\rangle\|^2\tau - \gamma_2\|\sigma_-|\psi_1\rangle\|^2\tau] \\ &= 1 - \exp[-\gamma_1c_2\tau - \gamma_2c_1\tau] \end{aligned} \quad (4.16)$$

For the strong coupling regimes the total waiting time distribution is

$$F(\tau) = 1 - \exp\left[2 \int_0^\tau dt_1 h(\tau - t_1)(-\gamma_1c_2\tau - \gamma_2c_1\tau)\right]. \quad (4.17)$$

The integrand of this equation is

$$\int_0^\tau dt_1 h(\tau - t_1) = \int_0^\tau dt_1 \frac{\delta\epsilon \sin^2(\delta\epsilon t/2)}{2\pi (\delta\epsilon t/2)^2}. \quad (4.18)$$

Use $\sin^2(\delta\epsilon t/2) = \frac{1}{2}(1 - \cos 2(\frac{\delta\epsilon t}{2})) = \frac{1}{2}(1 - \cos(\delta\epsilon t))$ and put it in Eq. (4.18)

$$\begin{aligned} \int_0^\tau dt_1 h(\tau - t_1) &= \frac{2}{\pi\delta\epsilon} \int_0^\tau dt_1 \frac{1}{2} \frac{(1 - \cos \delta\epsilon t)}{t^2} \\ &= \frac{1}{\pi\delta\epsilon} \int_0^\tau dt_1 \frac{(1 - \cos \delta\epsilon t)}{t^2} \\ &= \frac{1}{\pi\delta\epsilon} \left[\int_0^\tau \frac{1}{t^2} dt_1 - \int_0^\tau \frac{\cos \delta\epsilon t}{t^2} dt_1 \right]. \\ &= \frac{1}{\pi\delta\epsilon} \left[-\frac{1}{\tau} - \int_0^\tau \frac{\cos \delta\epsilon t}{t^2} dt_1 \right]. \end{aligned} \quad (4.19)$$

The second term requires an integration by part technique.

$$\int_0^\tau \frac{\cos \delta\epsilon t}{t^2} dt_1 = -\frac{\cos \delta\epsilon \tau}{\tau} - \int_0^\tau \frac{\delta\epsilon \sin \delta\epsilon t}{t} dt_1. \quad (4.20)$$

Substitutes Eq. (4.20) in Eq. (4.19) expands to

$$\int_0^\tau dt_1 h(\tau - t_1) = \frac{1}{\pi\delta\epsilon} \left[-\frac{1}{\tau} + \frac{\cos \delta\epsilon \tau}{\tau} + \int_0^\tau \frac{\delta\epsilon \sin \delta\epsilon t}{t} dt_1 \right]. \quad (4.21)$$

Substitutes Eq. (4.21) to Eq. (4.17) and obtain

$$F(\tau) = 1 - \exp \left[\frac{2[-1 + \cos(\delta\epsilon\tau) + \delta\epsilon\tau Si(\delta\epsilon\tau)]}{\delta\epsilon\tau\pi} \times (-\gamma_1 c_1 \tau - \gamma_2 c_1 \tau) \right], \quad (4.22)$$

where $Si(\delta\epsilon\tau) = \int_0^\tau \frac{\delta\epsilon \sin \delta\epsilon t}{t} dt_1$.

For the special cases, we first chose $a_1 = 1, b_1 = 0, a_2 = 0$ and $b_2 = 0$, then the jumps were found to be

$$|\psi_1\rangle = \begin{pmatrix} 1 \\ 0 \end{pmatrix}, |\psi_2\rangle = \begin{pmatrix} 0 \\ 0 \end{pmatrix}. \quad (4.23)$$

When $c_1 = 1$ and $c_2 = 0$, then the realisations are

$$|\tilde{\psi}_1\rangle \rightarrow \begin{pmatrix} 1 \\ 0 \end{pmatrix} |\tilde{\psi}_2\rangle \rightarrow \begin{pmatrix} 0 \\ 0 \end{pmatrix}. \quad (4.24)$$

The waiting time for the first jump in a weak coupling regime is

$$\eta_1 = e^{-\gamma_2 t} \Rightarrow \tau_1 = \frac{1}{\gamma_2} \ln \eta_1, \quad (4.25)$$

where $\eta_1 = \exp[-\gamma_1 c_2 \tau - \gamma_2 c_1 \tau]$ in Eq. (4.16).

For the second case, we chose $a_1 = 0, b_1 = 0, a_2 = 0$ and $b_2 = 1$, then the jumps were found to be

$$|\psi_1\rangle = \begin{pmatrix} 0 \\ 0 \end{pmatrix}, |\psi_2\rangle = \begin{pmatrix} 0 \\ 1 \end{pmatrix}. \quad (4.26)$$

When $c_1 = 0$ and $c_2 = 1$, then the realisations are

$$|\tilde{\psi}_1\rangle \rightarrow \begin{pmatrix} 0 \\ 0 \end{pmatrix}, |\tilde{\psi}_2\rangle \rightarrow \begin{pmatrix} 0 \\ 1 \end{pmatrix}. \quad (4.27)$$

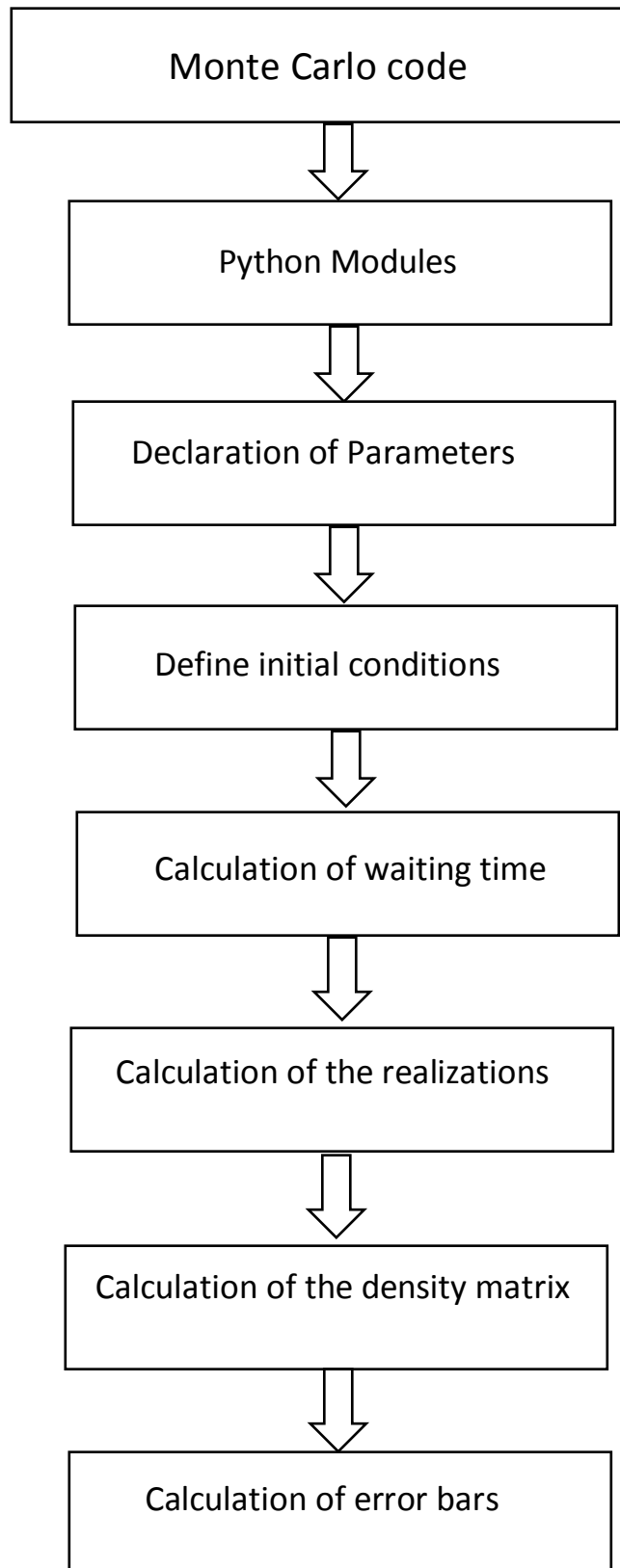
The waiting time for the next possible jump 2 in the weak coupling regime is

$$\eta_2 = e^{-\gamma_1 t} \Rightarrow \tau_2 = \frac{1}{\gamma_1} \ln \eta_2, \quad (4.28)$$

where $\eta_2 = \exp[-\gamma_1 c_2 \tau - \gamma_2 c_1 \tau]$ shown in Eq. (4.16). In a strong coupling regime $\eta_{1,2} = \exp\left[\frac{2[-1+\cos(\delta\epsilon\tau)+\delta\epsilon\tau Si(\delta\epsilon\tau)]}{\delta\epsilon\tau\pi} \times (-\gamma_1 c_1 \tau - \gamma_2 c_2 \tau)\right]$. It should be noted that for the strong coupling regime, the waiting times τ are extracted from the polynomial interpolation algorithm [19]. The description of how the populations and the coherences are undertaken in the Monte Carlo simulation has been shown in the results and discussion chapter.

4.2 Monte Carlo code Flow Chart

The following flow chart shows 7 steps which were followed in simulating our two level system coupled with an environment. The first step (Python modules) calls all the required modules that are built in functions in python. The second step (declaration of parameters) shows different chosen values for both regimes. The third step (initial condition) is where the initial conditions are defined. The total waiting time distribution is calculated in the fourth step. The realizations are calculated in fifth step. Immediately after this step, a density matrix and error bars are calculated in the sixth and seventh steps respectively. The complete codes which is complemented by this flow chart can be found on the appendix section.



Chapter 5

Results and discussions

5.1 Pure state

The results presented show two regimes that were investigated namely the weak coupling and strong coupling. In both of these regimes N_1 , N_2 , and $\delta\epsilon$ were varied interchangeably and the populations of the system were plotted. The comparison of the analytical solution of the second order time convolutionless (TCL2) solution for both time dependent and independent approaches was made with the Monte Carlo (MC) simulation. If the initial conditions $\rho_{11}(0) = 1$ and $\rho_{22}(0) = 0$ are substituted in Eqs. (3.16-3.19), and we consider $\gamma_1 = \gamma_2 = \gamma$, then the MC simulations are compared to the second order time convolutionless (TCL2) with a time-independent rate:

$$\rho_{ii}(t) = \frac{1}{2} \pm \frac{1}{2} e^{-2\gamma t}. \quad (5.1)$$

The index $i = 1$ corresponds to '+' and $i = 2$ corresponds to '-'. If the '+' sign is used in the TCL2 equation, then the lower level is populated denoted by ρ_{11} and if the '-' sign is used in the TCL2, then the upper level is populated denoted by ρ_{22} . If the initial conditions are now substituted in Eqs. (3.22-3.23), and with $\gamma_1 = \gamma_2 = \gamma$, then the MC simulations are compared to second order time convolutionless (TCL2(t)) solution with a time-dependent rate:

$$\rho_{jj}(t) = \frac{1}{2} \pm \frac{1}{2} e^{-2\Gamma(t)}. \quad (5.2)$$

The index $j = 1$ is for '+' and $j = 2$ is for '-'. If the '+' sign is used then the lower level is populated, and is denoted by ρ_{11} . The '-' sign is used in the TCL2 equation when the upper level is populated denoted by ρ_{22} . Here $\Gamma(t)$ is treated the same as Eq. (3.26). For both regimes 5000 trajectories were used in the Monte Carlo simulations to recover the quantum master equation.

5.1.1 Weak coupling results

Fig. 5.1 shows the population for the ground state where $N_1 = N_2 = 200$, $\delta\epsilon = 0.31$, and $\lambda = 0.001$. The comparison of TCL2, TCL2(t), and MC simulations is made. It is seen that MC, TCL2, and TCL2(t) are in good agreement with each other. Figs. 5.2 and 5.3 show the populations for the ground state and excited state respectively. In these figures, the number of levels N_1 and N_2 were uniformly varied. The energy band width $\delta\epsilon$, and the coupling strength λ were fixed at 0.31 and 0.001 respectively. These values were selected to satisfy the required condition for the weak coupling mentioned in the earlier chapter of this dissertation. The ground state of the system started fully populated i.e, $\rho_{11} = 1$, while excited state is $\rho_{22} = 0$. It has been observed that as time evolves, both states thermalize to the steady state where both ρ_{11} and ρ_{22} are equal to 0.5. It can be seen from Figs. 5.2 and 5.3 that as the number of levels N_1 and N_2 are increased simultaneously, both states thermalize to the steady state faster. Figs. 5.4 and 5.5 show the populations for the ground state and excited state respectively, where the energy band width $\delta\epsilon$ was varied. Here number of levels N_1 and N_2 , and the coupling strength λ were fixed at 150 and 0.001 respectively. The ground state of the system started fully populated i.e, $\rho_{11} = 1$, while the excited state is $\rho_{22} = 0$. Again it was observed that as time evolves, both states thermalize to steady state where both ρ_{11} and ρ_{22} are equal to 0.5. These figures show that as the energy band width $\delta\epsilon$ is increased, then both states take longer to thermalize to the steady state. Figs. 5.6 and 5.7 show the populations for the ground state and excited state respectively where N_1 was varied to very large values while N_2 was kept fixed at 150. The energy band width $\delta\epsilon$, and the coupling strength λ were fixed at 0.31, and 0.001 respectively. The ground state started fully populated i.e, $\rho_{11} = 1$, while the excited state $\rho_{22} = 0$. The figures show that as time evolves, both bands thermalize to different steady

states. In Fig. 5.6, as N_1 is increased to very large values, ρ_{11} thermalizes close to its initial state ($\rho_{11} = 1$). In Fig. 5.7, as N_1 is increased to very large values, ρ_{22} thermalizes close to its initial state ($\rho_{22} = 0$). The significance of these figures indicate controllability of the system. The controllability of the system was further investigated as shown in Figs. 5.8 and 5.9. In these figures, N_2 was varied to very large values while keeping N_1 fixed at 150. The energy band width $\delta\epsilon$, and the coupling strength λ were fixed at 0.31, and 0.001 respectively. The ground state started fully populated i.e, $\rho_{11} = 1$, while the excited state is $\rho_{22} = 0$. In Fig. 5.8, as N_2 is increased to very large values, ρ_{11} thermalizes close to the ground state ($\rho_{11} = 0$). In Fig. 5.9, as N_2 is increased to very large values, ρ_{22} thermalizes close to the excited state ($\rho_{22} = 1$). This again verifies that a system is controllable from one state to another state.

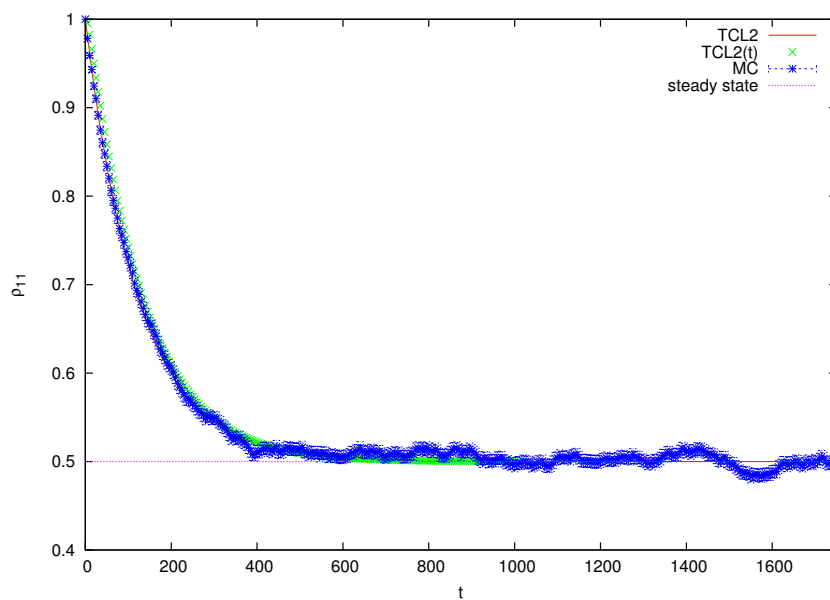


Figure 5.1: The ground state population for $N_1 = N_2 = 200$ with $\lambda = 0.001$ and $\delta\epsilon = 0.31$.

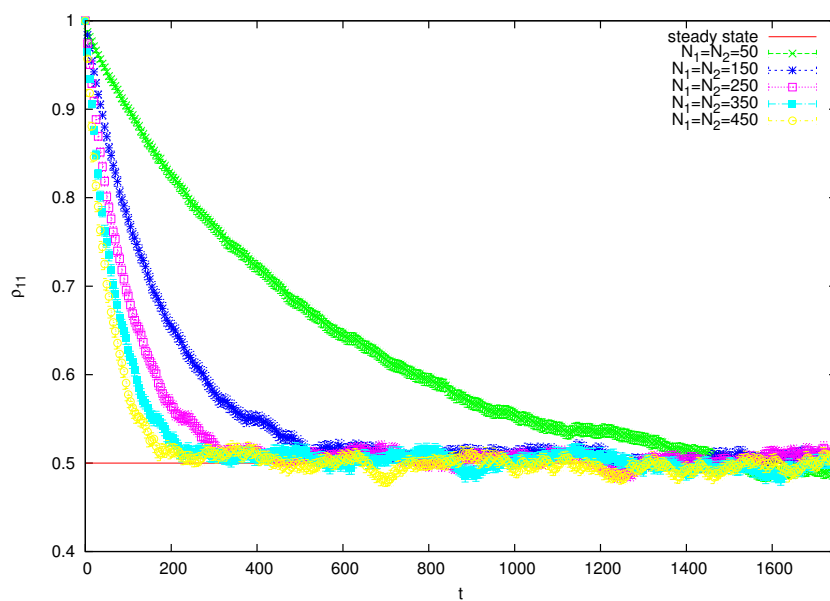


Figure 5.2: The ground state populations for variation of N_1 and N_2 with $\lambda = 0.001$ and $\delta\epsilon = 0.31$.

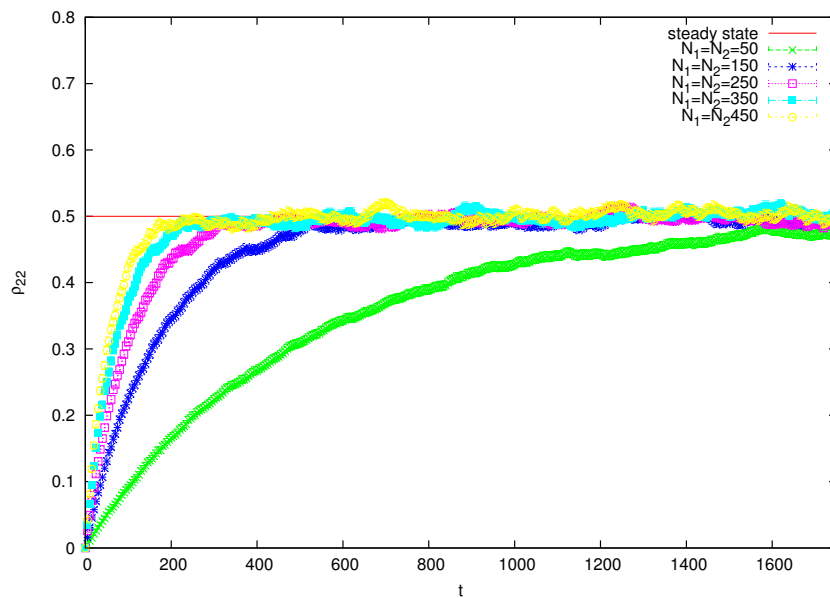


Figure 5.3: The excited state populations for variation of N_1 and N_2 with $\lambda = 0.001$ and $\delta\epsilon = 0.31$.

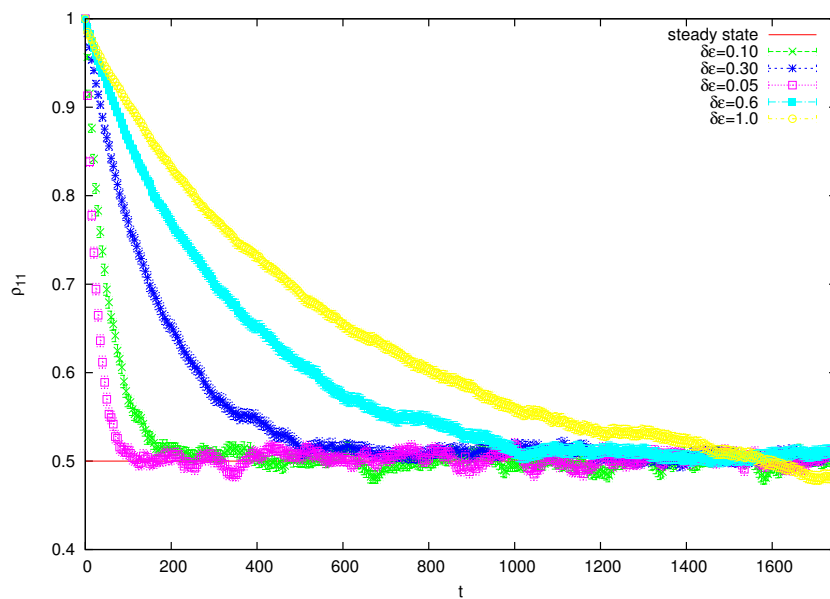


Figure 5.4: The ground state populations for variation of $\delta\epsilon$ with $N_1 = N_2 = 150$ and $\lambda = 0.001$.

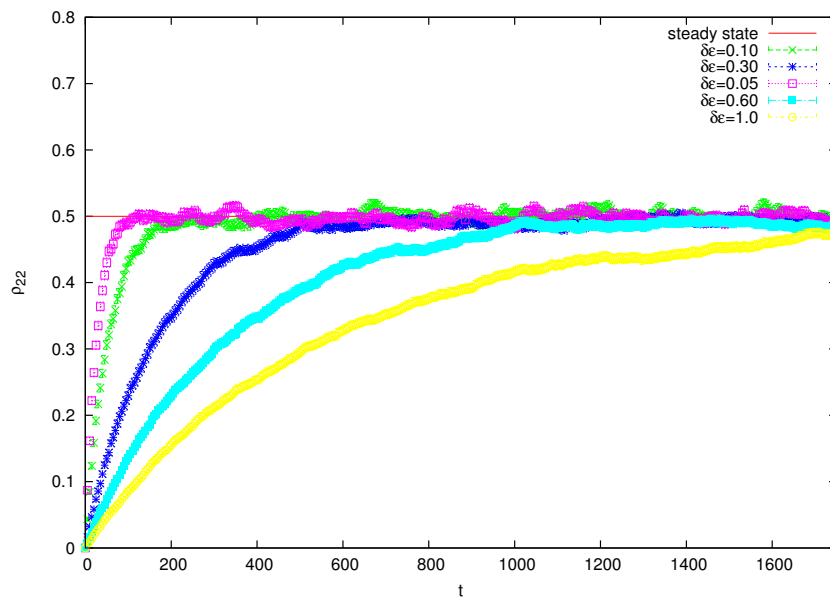


Figure 5.5: The excited state populations for variation of $\delta\epsilon$ with $N_1 = N_2 = 150$ and $\lambda = 0.001$.

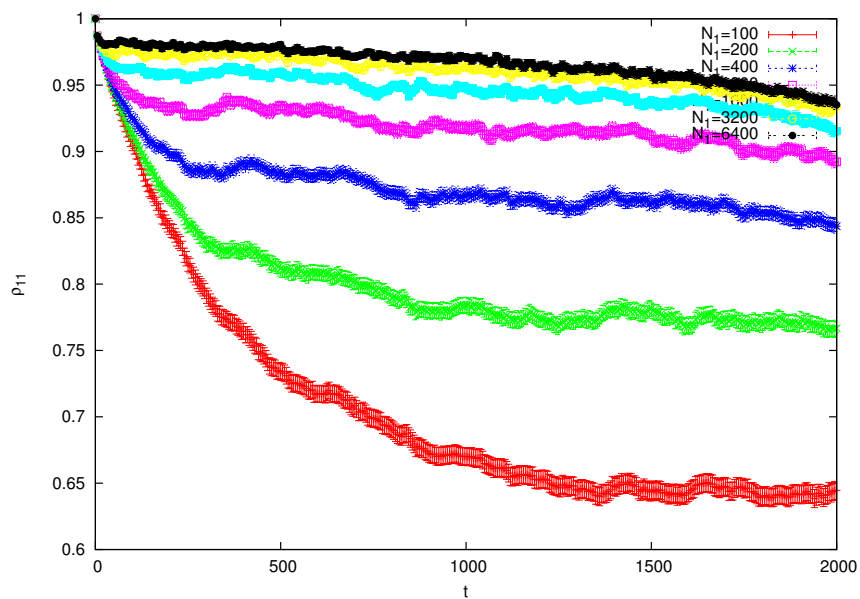


Figure 5.6: The ground state populations for variation of N_1 with $N_2 = 150$, $\lambda = 0.001$, and $\delta\epsilon = 0.31$.

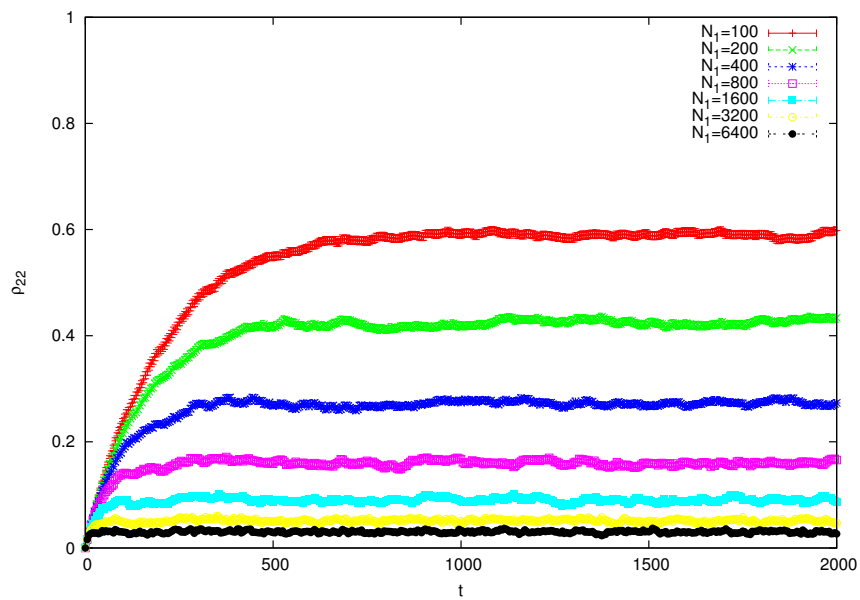


Figure 5.7: The excited state populations for variation of N_1 with $N_2 = 150$, $\lambda = 0.001$, and $\delta\epsilon = 0.31$.

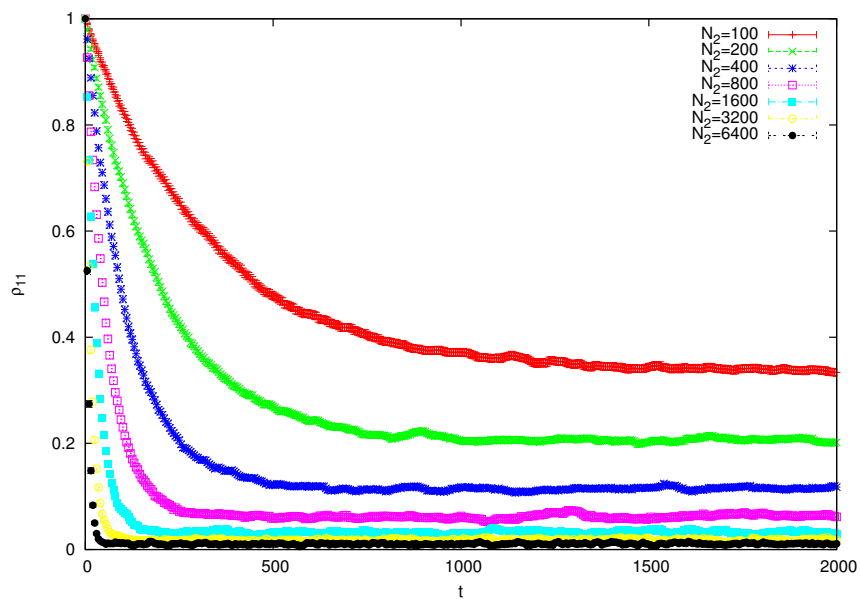


Figure 5.8: The ground state populations for variation of N_2 with $N_1 = 150$, $\lambda = 0.001$, and $\delta\epsilon = 0.31$.

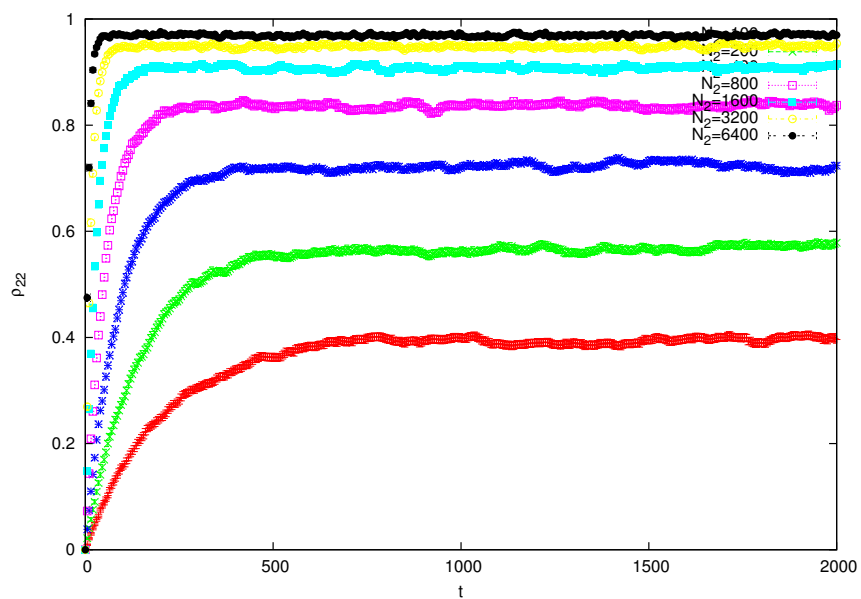


Figure 5.9: The excited state populations for variation of N_2 with $N_1 = 150$, $\lambda = 0.001$, and $\delta\epsilon = 0.31$.

5.1.2 Strong coupling results

Fig. 5.10 shows the population for the ground state where $N_1 = N_2 = 200$, $\delta\epsilon = 0.31$, and $\lambda = 0.01$. A comparison between TCL2, TCL2(t), and the MC simulations is made. Here it is seen that MC simulation, and TCL2(t) solution are in good agreement with each other, TCL2 solution on the other hand does not overlap the others. The reason for this is that the TCL2 was derived for the weak coupling. Figs. 5.11 and 5.12 show the populations for the ground state and excited state respectively. In these figures, the number of levels N_1 and N_2 were uniformly varied. The energy band width $\delta\epsilon$, and the coupling strength λ were fixed at 0.31 and 0.01 respectively. The ground state of the system started fully populated i.e, $\rho_{11} = 1$, while the excited state is $\rho_{22} = 0$. It has been observed that as time evolves, both states thermalize to the steady state where both ρ_{11} and ρ_{22} are equal to 0.5. It can be seen from Figs. 5.11 and 5.12 that as the number levels N_1 and N_2 are increased simultaneously, both states thermalize to the steady state faster. Figs. 5.13 and 5.14 show the populations for the ground state and excited state respectively, where the energy band width $\delta\epsilon$ was varied. Here the number of levels N_1 and N_2 , and the coupling strength λ were fixed at 150 and 0.01 respectively. The ground state of the system started fully populated i.e, $\rho_{11} = 1$, while excited state is $\rho_{22} = 0$. Again it has been observed that as time evolves, both states thermalize to steady state where both ρ_{11} and ρ_{22} are equal to 0.5. These figures show that as energy band width $\delta\epsilon$ is increased, then both states take longer to thermalize to the steady state. Figs. 5.15 and 5.16 show the populations for the ground state and excited state respectively, where N_1 was varied to very large values while N_2 was kept fixed at 150. The energy band width $\delta\epsilon$, and the coupling strength λ were fixed at 0.31, and 0.01 respectively. The ground state started fully populated i.e, $\rho_{11} = 1$, while excited state is $\rho_{22} = 0$. The figures show that as time evolves, both states thermalize to different steady states. In Fig. 5.15, as N_1 is increased to very large values, ρ_{11} thermalizes close to its initial state ($\rho_{11} = 1$). In Fig. 5.16 as N_1 is increased to very large values, then ρ_{22} thermalizes close to its initial state ($\rho_{22} = 0$). The significance of these figures indicate controllability of the system. The controllability of the system was further investigated as shown in Figs. 5.17 and 5.18. In these figures, N_2 was varied to very large values while keeping N_1 fixed at 150. The energy band width $\delta\epsilon$, and the coupling strength λ were

fixed at 0.31, and 0.001 respectively. The ground state started fully populated i.e, $\rho_{11} = 1$, while the excited state is $\rho_{22} = 0$. In Fig. 5.17, as N_2 is increased to very large values, ρ_{11} thermalizes close to the ground state ($\rho_{11} = 0$). In Fig. 5.18, as N_2 is increased to very large values, then ρ_{22} thermalizes close to the excited state ($\rho_{22} = 1$). This again verifies that a system is controllable from one state to another state.

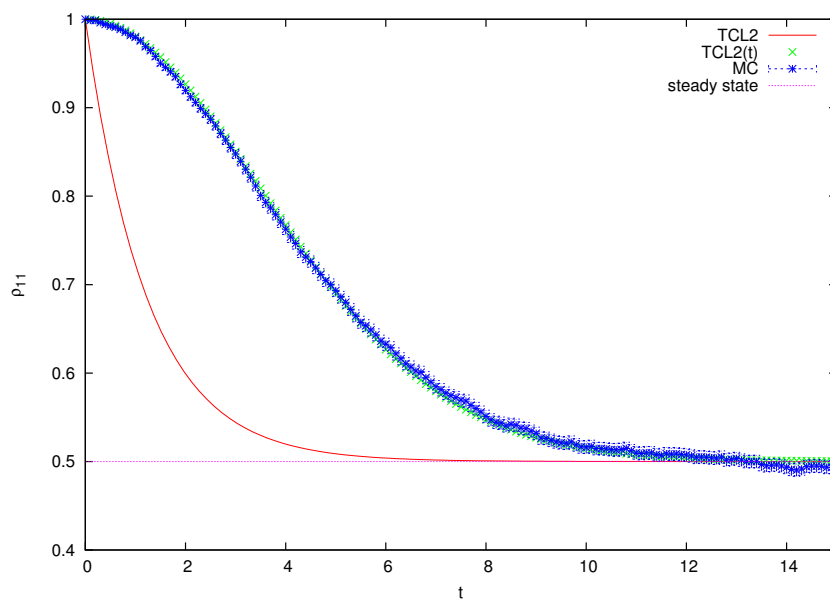


Figure 5.10: The ground state population for $N_1 = N_2 = 200$ with $\delta\epsilon = 0.31$, and $\lambda = 0.01$.

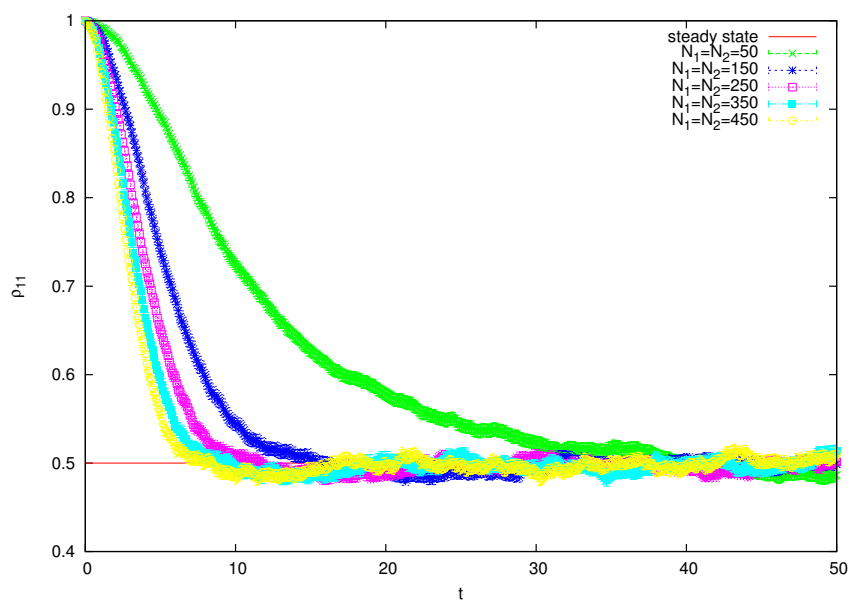


Figure 5.11: The ground state populations for variation of N_1 and N_2 with $\delta\epsilon = 0.31$, and $\lambda = 0.01$.

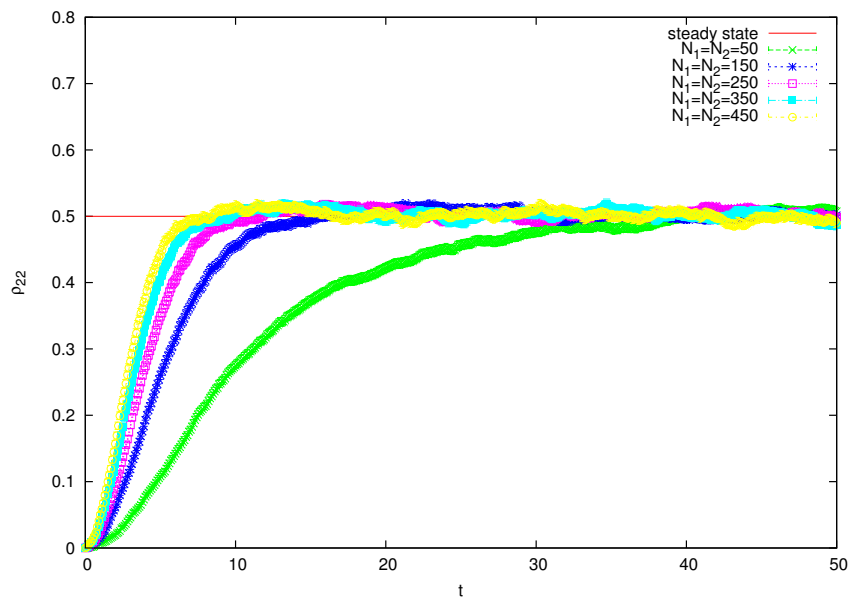


Figure 5.12: The excited state populations for variation of N_1 and N_2 with $\delta\epsilon = 0.31$, and $\lambda = 0.01$.

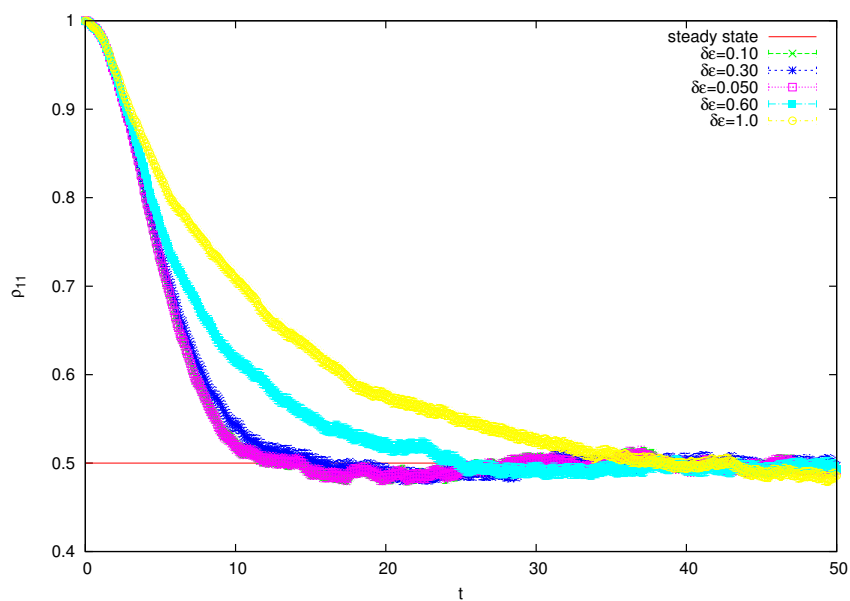


Figure 5.13: The ground state populations for variation of $\delta\epsilon$ with $N_1 = N_2 = 150$, and $\lambda = 0.01$.

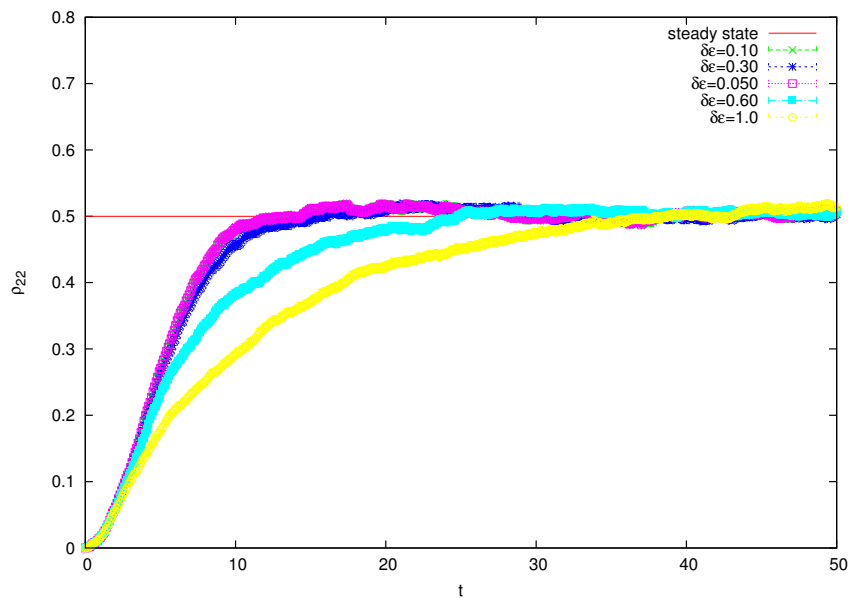


Figure 5.14: The excited state populations for variation of $\delta\epsilon$ with $N_1 = N_2 = 150$, and $\lambda = 0.01$.

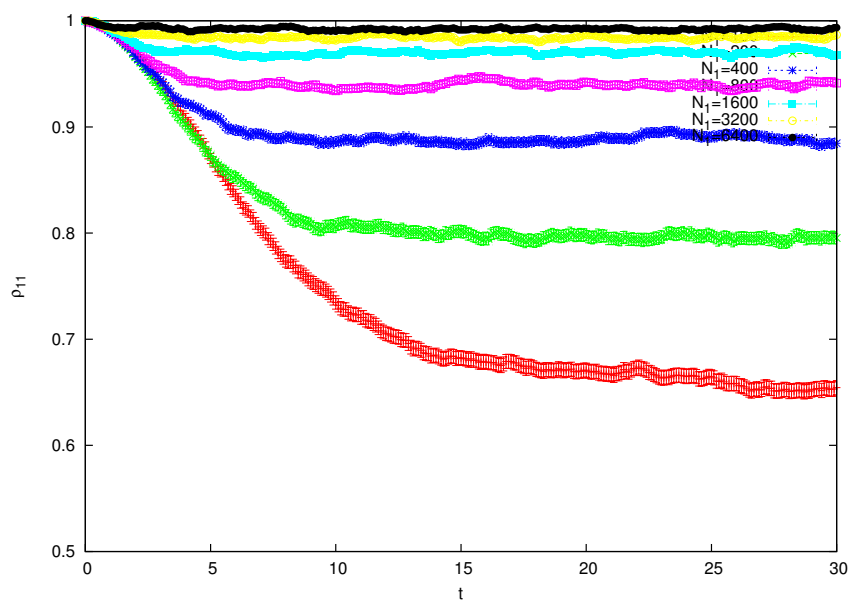


Figure 5.15: The ground state populations for variation of N_1 with $N_2 = 150$, $\delta\epsilon = 0.31$, and $\lambda = 0.01$.

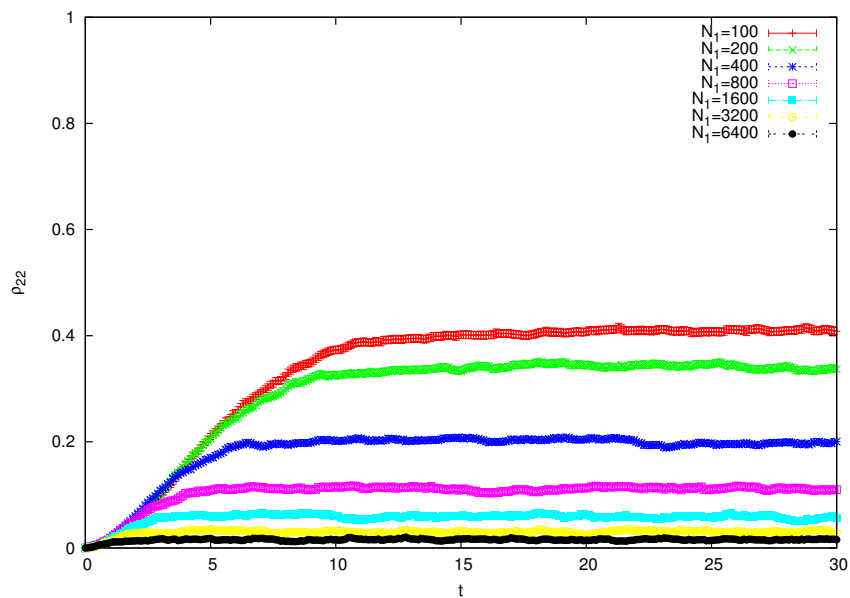


Figure 5.16: The excited state populations for variation of N_1 with $N_2 = 150$, $\delta\epsilon = 0.31$, and $\lambda = 0.01$.

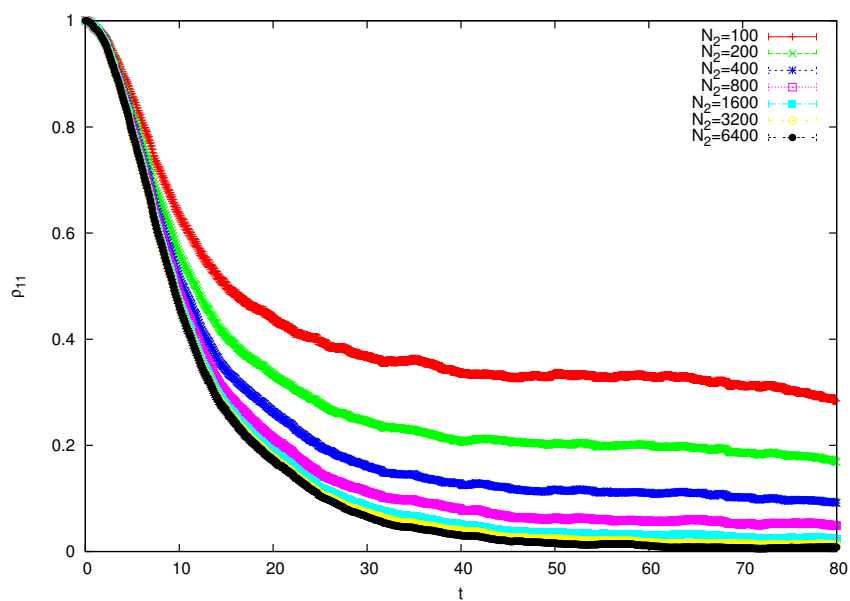


Figure 5.17: The ground state populations for variation of N_2 with $N_1 = 150$, $\delta\epsilon = 0.31$, and $\lambda = 0.01$.

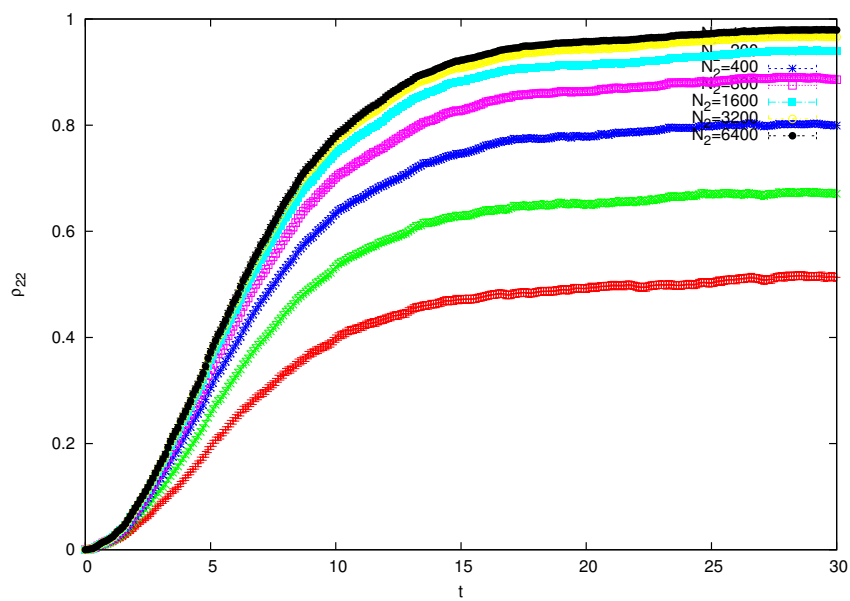


Figure 5.18: The excited state populations for variation of N_2 with $N_1 = 150$, $\delta\epsilon = 0.31$, and $\lambda = 0.01$.

5.2 Correlated state

The correlated state is defined such that it is a combination of the system state vectors and the environment population [2]. Using such a state we can investigate our model with a initial state that has both energy bands populated. The initial state is given by

$$|\psi(0)\rangle = \sqrt{\beta}|g\rangle + \sqrt{1-\beta}e^{i\phi}|e\rangle. \quad (5.3)$$

Here β is a population ratio of the lower band and $1-\beta$ is a population of the upper band. They are defined as

$$\beta = \frac{\text{tr}_E\{\Pi_1\rho_E(0)\}}{N_1}, \quad (5.4)$$

and

$$1-\beta = \frac{\text{tr}_E\{\Pi_2\rho_E(0)\}}{N_2}. \quad (5.5)$$

The population ratio (β) can take any value in the interval $[0, 1]$. If $\beta = 1$, then Eq. (5.4) only survives and this means that the lower band ($\frac{\text{tr}_E\{\Pi_1\rho_E(0)\}}{N_1} = 1$) is only populated. If $\beta = 0$, then Eq. (5.5) only survives and thus the upper band ($\frac{\text{tr}_E\{\Pi_2\rho_E(0)\}}{N_2} = 1$) is only populated. If $\beta = 0.5$ both lower and upper bands are equally populated. The ϕ represents the azimuthal angle which is associated to a state vector on the Bloch sphere. The initial conditions used to simulate the populations are

$$\rho_{11}(0) = \beta \quad (5.6)$$

$$\rho_{22}(0) = 1 - \beta. \quad (5.7)$$

and for the coherence terms

$$\rho_{12}(0) = \rho_{21}(0) = \sqrt{\beta(1-\beta)}. \quad (5.8)$$

If these conditions are substituted in Eqs. (3.16-3.19), and we consider in Eq. (3.12) that $N_1 = N_2$, then $\gamma_1 = \gamma_2 = \gamma$. The second order time convolutionless (TCL2) with time-independent rate population is then going to be

$$\rho_{uu}(t) = \frac{1}{2} \pm \left[\beta - \frac{1}{2} \right] e^{-2\gamma t}, \quad (5.9)$$

and the coherences

$$\rho_{lm}(t) = \frac{1}{2} \sqrt{\beta(1-\beta)} [1 + e^{-2\gamma t}]. \quad (5.10)$$

The index $l = 1$ corresponds to '+' and $l = 2$ corresponds to '-' and for the coherences l and m equal to 1 or 2 but $l \neq m$. If these conditions are now substituted in Eqs. (3.22-3.23), and considering that $\gamma_1 = \gamma_2$, then the simulation of the second order time convolutionless (TCL2(t)) with time-dependent rate population is

$$\rho_{ll}(t) = \frac{1}{2} \pm \left[\beta - \frac{1}{2} \right] e^{-2\Gamma(t)} \quad (5.11)$$

and the coherence term is

$$\rho_{lm}(t) = \frac{1}{2} \sqrt{\beta(1-\beta)} [1 + e^{-2\Gamma(t)}]. \quad (5.12)$$

The index l and m have the same interpretation as mentioned above. Here $\Gamma(t)$ is treated the same as Eq. (3.26). Eqs. (5.10) and (5.12) represent off-diagonal terms of the reduced density matrix (coherences). The MC simulation as discussed in Chapter 4 was again used to simulate Eqs. 5.11 and 5.12. For both strong and weak coupling regimes 5000 trajectories were used in the Monte Carlo simulations.

5.2.1 Weak coupling results

Figs. 5.19 and 5.20 show the populations for the ground state and excited state where the number levels $N_1 = N_2 = N$ are varied as 100, 200, 400, and 800. The energy band width is $\delta\epsilon = 0.31$, and the coupling strength is $\lambda = 0.001$. These figures are plotted for the different values of the environment population ratio β . The comparison of the TCL2 approximation mentioned in Eq. (5.9) with MC simulations is made. It can be seen that both solutions overlap completely. If $\beta = 1$, then Fig. 5.19 shows $\rho_{11}(0) = 1$, while Fig. 5.20 shows $\rho_{22}(0) = 0$. As time evolves, both states populate to 0.5. If $\beta = 0$, Fig. 5.19 shows $\rho_{11}(0) = 0$, while Fig. 5.20 shows $\rho_{22}(0) = 1$. As time evolves, then both states populate to 0.5. It can be seen from Figs. 5.19 and 5.20, as the number levels are increased simultaneously, both states thermalize to the steady state faster. Figs. 5.21 and 5.22 show the coherences (off diagonal terms of a density matrix) of the system. In Fig. 5.21 shows the plot for $N_1 = N_2 = N = 100$, while $\delta\epsilon = 0.31$, and $\lambda = 0.001$. In this

figure the MC simulation was compared to TCL2 solution and the overlap of the trends were obtained. Fig. 5.21 also shows coherences thermalizing at the same time but having different values of population ratios. In Fig. 5.22 is when number of levels are varied, while $\delta\epsilon = 0.31$, and $\lambda = 0.001$. We have chosen $\beta = 0.5$, and observed that as number level increases then ρ_{12} reaches the steady states faster.

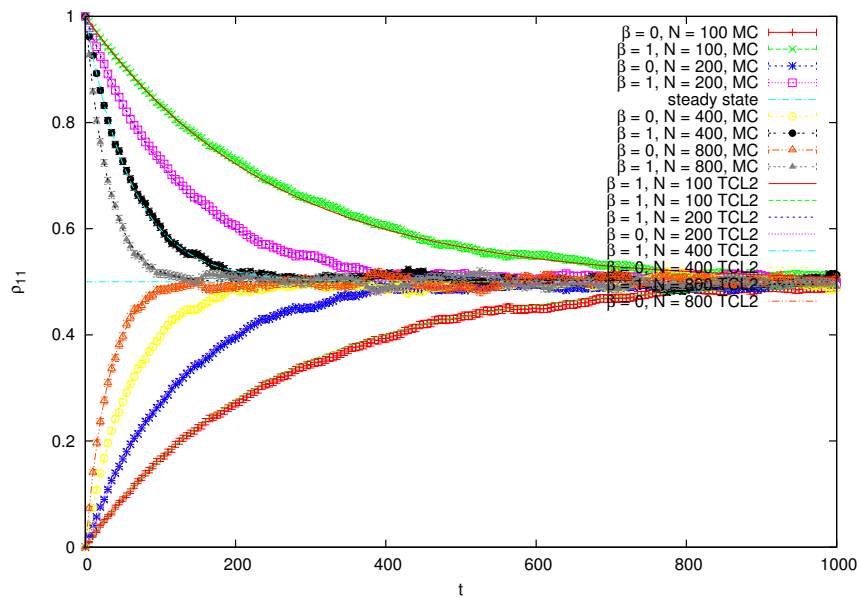


Figure 5.19: The ground state population for the variation of energy levels $N_1 = N_2 = N$ with $\delta\epsilon = 0.31$, and $\lambda = 0.001$.

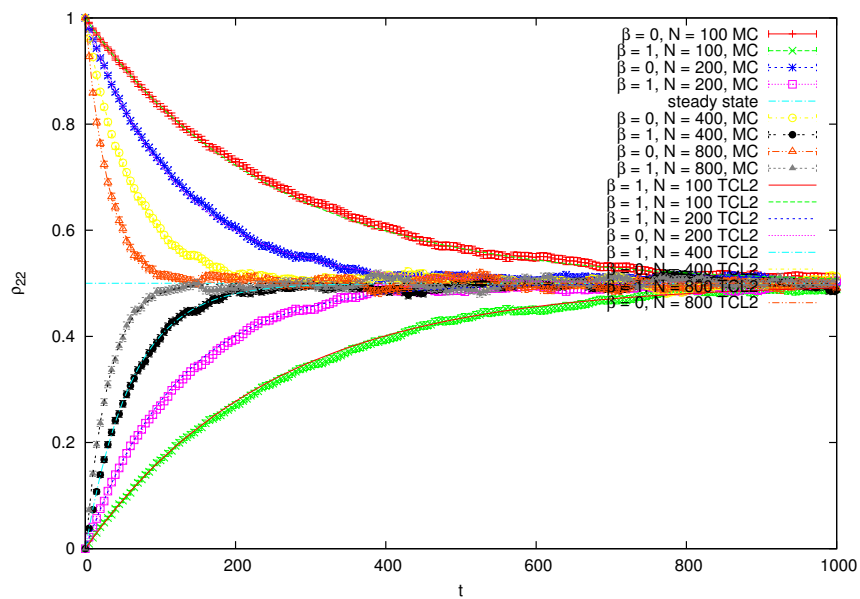


Figure 5.20: The excited state population for the variation of number levels $N_1 = N_2 = N$ with $\delta\epsilon = 0.31$, and $\lambda = 0.001$.

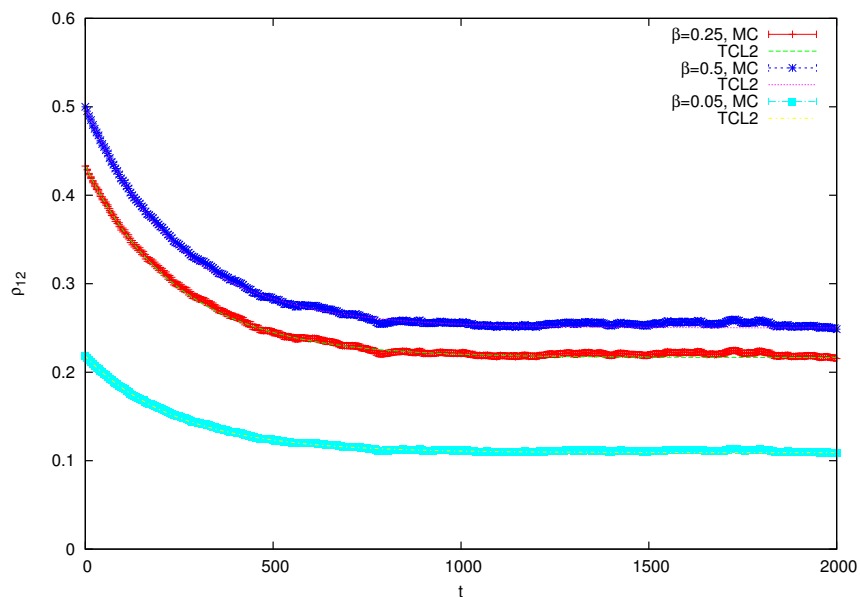


Figure 5.21: The coherences for $N_1 = N_2 = 100$ with $\delta\epsilon = 0.31$, and $\lambda = 0.001$.

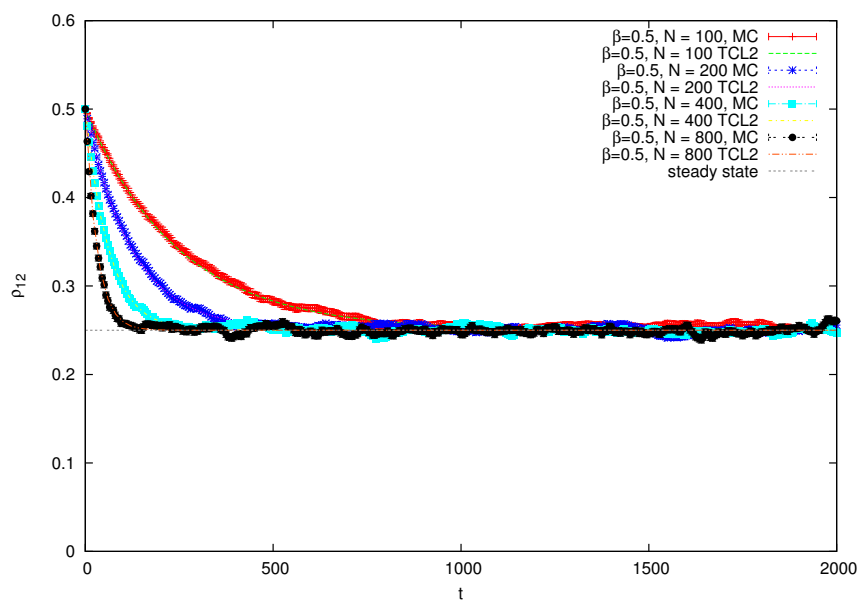


Figure 5.22: The coherences for the variation of number levels $N_1 = N_2 = N$ with $\delta\epsilon = 0.31$, and $\lambda = 0.001$.

5.2.2 Strong coupling results

Figs. 5.23 and 5.24 show the populations for the ground state and excited state where the number levels $N_1 = N_2 = N$ are varied as 100, 200, 400, and 800. The energy band width is $\delta\epsilon = 0.31$, and the coupling strength is $\lambda = 0.001$. These figures are plotted for the different values of the environment population ratio β . The comparison of the TCL2(t) approximation mentioned in Eq. (5.11) with MC simulations is made. It can be seen that both solutions overlap completely. If $\beta = 1$, then Fig. 5.23 shows $\rho_{11}(0) = 1$, while Fig. 5.24 shows $\rho_{22}(0) = 0$. As time evolves, both states populate to 0.5. If $\beta = 0$, Fig. 5.23 shows $\rho_{11}(0) = 0$, while Fig. 5.24 shows $\rho_{22}(0) = 1$. As time evolves, then both states populate to 0.5. It can be seen from Figs. 5.23 and 5.24, as the number levels are increased simultaneously, both states thermalize to the steady state faster. Figs. 5.25 and 5.26 show the coherences of the system. In Fig. 5.25 shows the plot for $N_1 = N_2 = N = 100$, while $\delta\epsilon = 0.31$, and $\lambda = 0.001$. In this figure the MC simulation was compared to TCL2(t) solution and the overlap of the trends were obtained. Fig. 5.25 also shows coherences thermalizing at the same time but having different values of population ratios. In Fig. 5.26 is when number of levels are varied, while $\delta\epsilon = 0.31$, and $\lambda = 0.001$. We have chosen $\beta = 0.5$, and observed that as number level increases then ρ_{12} reaches the steady states faster.

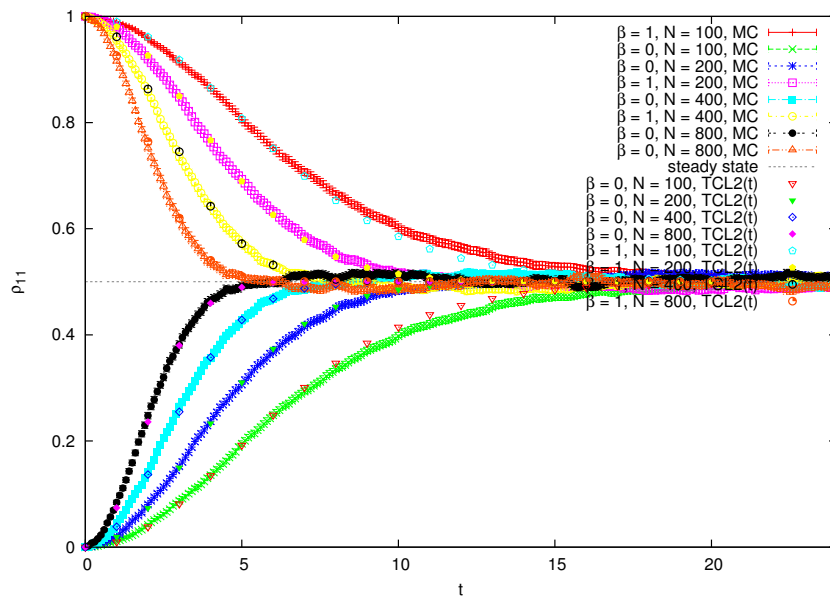


Figure 5.23: The ground state population for the variation of energy levels $N_1 = N_2 = N$ with $\delta\epsilon = 0.31$, and $\lambda = 0.001$.

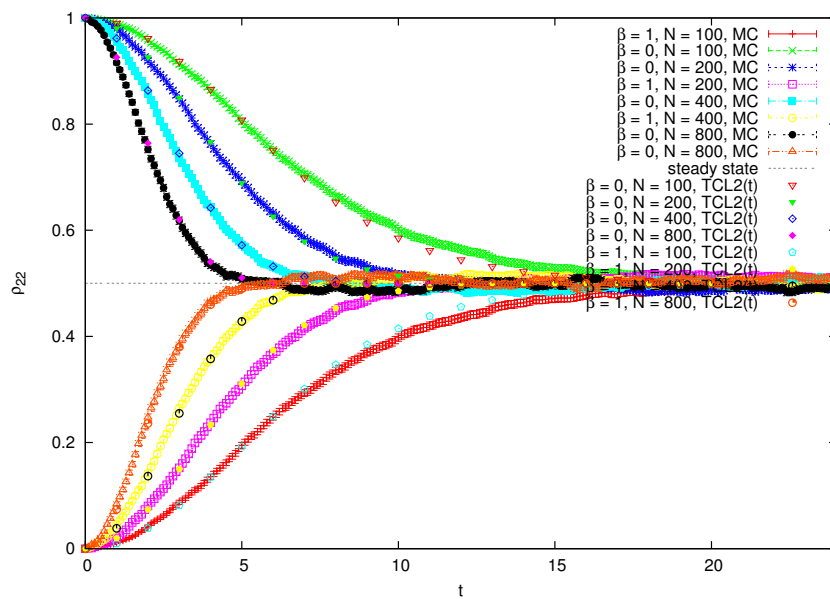


Figure 5.24: The excited state population for the variation of number levels $N_1 = N_2 = N$ with $\delta\epsilon = 0.31$, and $\lambda = 0.001$.

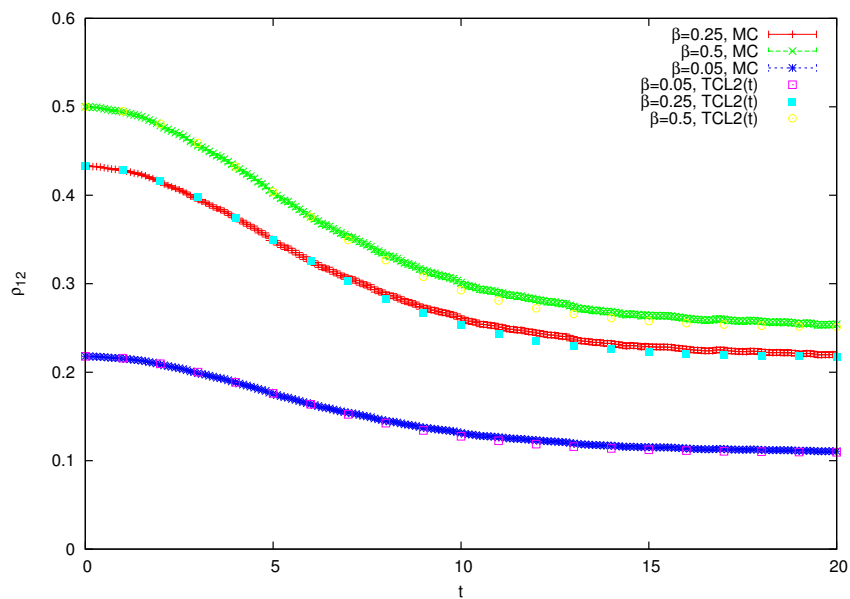


Figure 5.25: The coherences for $N_1 = N_2 = 100$ with $\delta\epsilon = 0.31$, and $\lambda = 0.001$.

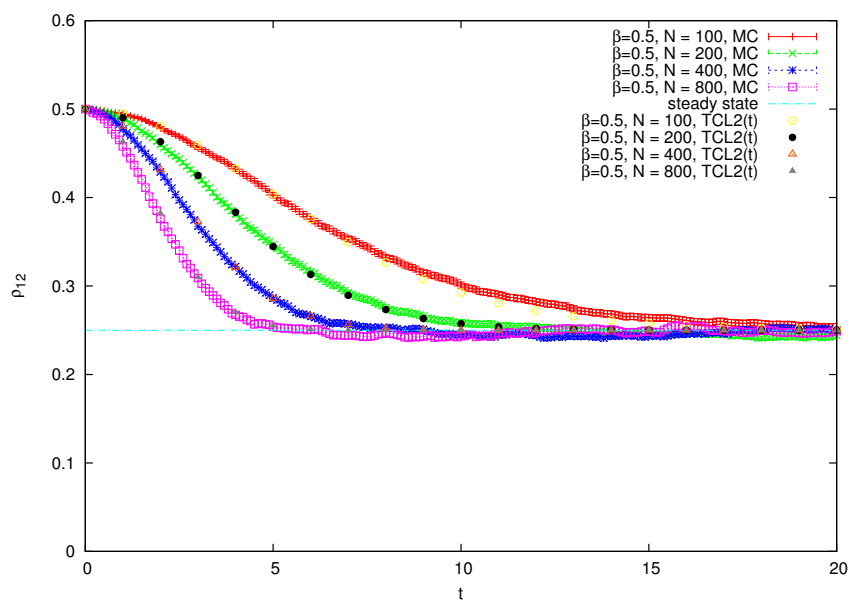


Figure 5.26: The coherences for the variation of number levels $N_1 = N_2 = N$ with $\delta\epsilon = 0.31$, and $\lambda = 0.001$.

Chapter 6

Conclusions

The dynamics of the two level system coupled both strongly and weakly to an environment were studied. The comparison of the Monte Carlo wave-function simulations (MC) was made with second order time convolutionless for both time-independent (TCL2) and time-dependent (TCL2(t)) simulations. It has be observed that all simulations (MC, TCL2, TCL2(t)) are in good agreement with one another in the weak coupling scenario, and only MC and TCL2(t) were only found to be in good correlation with one another in the strong coupling. This is due to the fact that the TCL2 was derived for the weak coupling case. For the pure state when energy levels $N_1 = N_2$ were uniformly increased while coupling strength λ and energy band width $\delta\epsilon$ were fixed both lower and upper bands took longer to thermalize (to reach a steady state $\rho_{11} = \rho_{22} = 0.5$). When the energy band width $\delta\epsilon$ was increased, while energy levels N_1 and N_2 coupling strength λ were fixed, both lower and upper bands took longer to reach the steady state. Another interesting observation was that ρ_{11} and ρ_{22} can be driven back to its initial state if N_1 is increased to large values while N_2 , λ , and $\delta\epsilon$ are kept unchanged. If N_2 is increased to large values while N_1 , λ , and $\delta\epsilon$ are kept unchanged, then ρ_{11} and ρ_{22} can be driven into the next state. In the correlated state $N_1 = N_2$ were the only parameters that were varied, and it was observed that as $N_1 = N_2$ increases then the system takes a shorter time to reach the steady state. For the future investigation, one can use large values of N_1 and N_2 to see if the system can remain at its initial state while interactiong with the environment.

Appendices

Appendix A

Monte Carlo codes

A.1 Weak coupling for pure state

```
### This part calls all the python modules and operations needed #####
from qutip import *
from scipy import *
from pylab import *
import random
import time

### The declaration of parameters and dimensions ###
start_time = time.time()
def run():
    n = 2          # number of states (ground and excited states)
    nnr = 5000    # Monte Carlo runs
    nt = 3000     # Monte Carlo times
    tau = zeros([1500+1])
    wfn1 = zeros((nnr+1,nt+1,n+1))
    wfn2 = zeros((nnr+1,nt+1,n+1))
    wfn1_new = zeros((nnr+1,nt+1,n+1))
```

```
wfn2_new = zeros((nnr+1,nt+1,n+1))
prodt = zeros((nnr+1,nt+1))
prodt_total = zeros((nt+1))
errt = zeros((nt+1))
rho = zeros((nnr+1,nt+1,n+1,n+1))
ira = 4321
N0 = 150          ## Environment energy levels
N1 = N0
N2 = N0
dlam = 0.001e00   # Coupling strength
dN1 = N1*1.0e00
dN2 = N2*1.0e00
d_e = 0.31        # Energy band width
gamma1 = 2.0*pi*dlam**2*dN1/d_e   # relaxation rates 1
gamma2 = 2.0*pi*dlam**2*dN2/d_e   # relaxation rates 2

for i in range(1,nnr+1):
    for j in range(0,nt+1):
        prodt[i,j]=0.0

for nr in range(1,nnr+1):

    quit = False
    skip = False
    ira = ira+1
    random.seed( ira )
    rn = random.random()
    t_ini = 0.0
    t_fin = 5000.0
    delta_t = 5.0
```

```

n_s = (t_fin-t_ini)/delta_t
s_n = int(n_s)
t_sum = 0.0
ntau_max = 100
n_ss_old = 0
tau[0] = 0.0

wfn1[nr, n_ss_old, 1] = 1.0
wfn1[nr, n_ss_old, 2] = 0.0
wfn2[nr, n_ss_old, 1] = 0.0
wfn2[nr, n_ss_old, 2] = 0.0

for m in range(1, ntau_max+1):
    quit = False
    skip = False

    rn = random.random()

    if (wfn1[nr, n_ss_old, 1]==1.0 and wfn1[nr, n_ss_old, 2]==0.0):
        tau[m] = (-1.0/gamma2)*log(rn)
    elif (wfn2[nr, n_ss_old, 1]==0.0 and wfn2[nr, n_ss_old, 2]==1.0
):
        tau[m] = (-1.0/gamma1)*log(rn) # Calculate waiting time

    if (tau[m]>t_fin):
        t_sum = t_fin
        quit = True
    else:
        t_sum = t_sum+tau[m]

```



```

if (t_sum>t_fin ):
    t_sum = t_fin
    quit = True
sn_ss = t_sum/delta_t
n_ss = int(sn_ss)
if (sn_ss != 0.0 and sn_ss-n_ss<0.5):
    n_ss = n_ss-1
elif (sn_ss==0.0):
    skip = True

for ntt in range(n_ss_old , n_ss+1):
    if (n_ss_old==0):
        wfn1 [nr , ntt , 1] = 1.0 # Initial value wave 1
        wfn1 [nr , ntt , 2] = 0.0 # Initial value wave 1
        wfn2 [nr , ntt , 1] = 0.0 # Initial value wave 2
        wfn2 [nr , ntt , 2] = 0.0 # Initial value wave 2
    else :
        wfn1 [nr , ntt , 1] = wfn1 [nr , n_ss_old , 1] # value after jump
        wfn1 [nr , ntt , 2] = wfn1 [nr , n_ss_old , 2] # value after jump
        wfn2 [nr , ntt , 1] = wfn2 [nr , n_ss_old , 1] # value after jump
        wfn2 [nr , ntt , 2] = wfn2 [nr , n_ss_old , 2] # value after jump
#### Calculate the realizations of wave 1 #####
if (wfn1 [nr , ntt , 1]==0.0 and wfn1 [nr , ntt , 2]==0.0):
    wfn1_new [nr , ntt , 1] = 0.0
    wfn1_new [nr , ntt , 2] = 0.0
elif (wfn1 [nr , ntt , 1]==1.0 and wfn1 [nr , ntt , 2]==0.0):
    wfn1_new [nr , ntt , 1] = 1.0
    wfn1_new [nr , ntt , 2] = 0.0
#### Calculate the realizations of wave 2 #####
if (wfn2 [nr , ntt , 1]==0.0 and wfn2 [nr , ntt , 2]==0.0):

```

```

        wfn2_new[nr, ntt, 1] = 0.0
        wfn2_new[nr, ntt, 2] = 0.0
    elif (wfn2[nr, ntt, 1]==0.0 and wfn2[nr, ntt, 2]==1.0):
        wfn2_new[nr, ntt, 1] = 0.0
        wfn2_new[nr, ntt, 2] = 1.0

##### Calculate the density matrix #####
rho[nr, ntt, 1, 1] = wfn1_new[nr, ntt, 1]**2
+ wfn2_new[nr, ntt, 1]**2
prodt[nr, ntt] = rho[nr, ntt, 1, 1]
if(skip):
    prodt[nr, 1] = 1.0
    break
if(quit):
    break

n_ss_old = n_ss+1
if (wfn1[nr, n_ss, 1]==0.0 and wfn1[nr, n_ss, 2]==0.0):
    wfn1[nr, n_ss_old, 1] = 1.0
    wfn1[nr, n_ss_old, 2] = 0.0
    wfn2[nr, n_ss_old, 1] = 0.0
    wfn2[nr, n_ss_old, 2] = 0.0
else:
    wfn1[nr, n_ss_old, 1] = 0.0
    wfn1[nr, n_ss_old, 2] = 0.0
    wfn2[nr, n_ss_old, 1] = 0.0
    wfn2[nr, n_ss_old, 2] = 1.0

for i in range(0, s-n+1):
    prodt_total[i] = 0.0
    for j in range(1, nnr+1):
        prodt_total[i] = prodt_total[i]+prodt[j, i]

```

```

##### Caluculate the statistics #####
for i in range(0,s_n+1):
    errt[i] = 0.0
    ttt = i*delta_t+t_ini
    for j in range(1,nnr+1):
        errt[i] = errt[i]+(prodt[j,i]-prodt_total[i]/nnr)**2
    print i, ttt, prodt_total[i]/nnr, sqrt(errt[i]/(nnr*(nnr-1)))
    txt = str(i) + '\t' + str(ttt) + '\t' + str(prodt_total[i]/nnr)
    + '\t' + str(sqrt(errt[i]/(nnr*(nnr-1)))) + '\n'
    file.write(txt)

file.close()

show()
close('all')

if __name__ == "__main__":
    run()
print ("---% seconds---"%(time.time() -start_time))

```

A.2 Strong coupling for pure state

```

### This part calls all the python modules and operations needed #####
from qutip import *
from scipy import *
from pylab import *
import random
import time

### The declaration of parameters and dimensions ###

```

```

start_time = time.time()
def run():
    n = 2          # number of states (ground and excited states)
    nnr = 5000    # Monte Carlo runs
    nt = 3000    # Monte Carlo times
    tau = zeros([1500+1])
    wfn1 = zeros((nnr+1,nt+1,n+1))
    wfn2 = zeros((nnr+1,nt+1,n+1))
    wfn1_new = zeros((nnr+1,nt+1,n+1))
    wfn2_new = zeros((nnr+1,nt+1,n+1))
    prodt = zeros((nnr+1,nt+1))
    prodt_total = zeros((nt+1))
    errt = zeros((nt+1))
    rho = zeros((nnr+1,nt+1,n+1,n+1))
    tt = zeros((10001+1))
    rnu = zeros((10001+1))
    t_t = zeros((5+1))
    rnuu = zeros((5+1))
    ira = 200
    N0 = 150          ## Environment energy levels
    N1 = N0
    N2 = N0
    dlam = 0.01e00   # Coupling strength
    dN1 = N1*1.0e00
    dN2 = N2*1.0e00
    d_e = 0.31       # Energy band width
    gamma1 = 2.0*pi*dlam**2*dN1/d_e   # Relaxation rate 1
    gamma2 = 2.0*pi*dlam**2*dN2/d_e   # Relaxation rate 2
    ##### This part calculate the sine integral and Gaussian quadrature
    for i in range(0,10000+1):

```

```

tt[i] = 0.5*i*pi/180.0
b = d_e*tt[i]
a = 0.0*pi/180.0
xm = 0.5*(b+a)
xr = 0.5*(b-a)
ee = d_e/2.0
w = zeros((5))
x = zeros((5))
w = [0,0.2955242274, 0.2692667193, 0.2190863625, 0.1494513491
, 0.0666713443]
x = [0,0.1488743389, 0.4333953941, 0.6794095682, 0.8650633666
, 0.9739065285]
ss = 0.0
for j in range(1,5+1):
    dx = xr*x[j]
    ss = ss+w[j]*(sin(xm+dx)/(xm+dx)+sin(xm-dx)/(xm-dx))
ss = xr*ss
tt[i] = 0.5*i*pi/180.0
h = (-1+cos(d_e*tt[i])+d_e*tt[i]*ss)/(d_e*tt[i]*pi)
rnu[i] = exp(-h*tt[i]*gamma1*2)
rnu[0] = 1.0

for i in range(1,nnr+1):
    for j in range(0,nt+1):
        prodt[i,j]=0.0

for nr in range(1,nnr+1):

    quit = False
    skip = False

```

```

ira = ira+1
random.seed( ira )
rn = random.random()
t_ini = 0.0
t_fin = 100.0
delta_t = 0.1
n_s = (t_fin-t_ini)/delta_t
s_n = int(n_s)
t_sum = 0.0
ntau_max = 100
n_ss_old = 0
tau[0] = 0.0

wfn1[nr, n_ss_old, 1] = 1.0 # Initial condition for wave 1
wfn1[nr, n_ss_old, 2] = 0.0 # Initial condition for wave 1
wfn2[nr, n_ss_old, 1] = 0.0 # Initial condition for wave 2
wfn2[nr, n_ss_old, 2] = 0.0 # Initial condition for wave 2

for m in range(1, ntau_max+1):
    quit = False
    skip = False

    rn = random.random()
#### This part interpolate the waiting function.
    for ii in range(0, 8500+1):
        if(rn < rnu[ii-1] and rn > rnu[ii]):
            break
    for j in range(0, 5+1):
        t_t[j] = tt[ii-1+j]
        rnuu[j] = rnu[ii-1+j]

```

```
if (t_t[0] > t_fin):
    tau[m] = t_t[0]

if (t_t[0] > t_fin):
    break
nmaxx = 10
n = 5
xa = rnuu
ya = t_t
c = zeros((nmaxx))
db = zeros((nmaxx))
ns = 1
x = rn
dif = abs(x-xa[1])

for i in range(1,n+1):
    dift = abs(x-xa[i])
    if (dift < dif):
        ns = i
        dif = dift

c[i] = ya[i]
db[i] = ya[i]

y = ya[ns]
ns = ns - 1

for m in range(1, (n-1)+1):
    for i in range(1, (n-m)+1):
        ho = xa[i]-x
```

```

        hp = xa [ i+m]-x
        w = c [ i+1]-db [ i ]
        den = ho-hp
        if (den==0.0):
            break
        den = w/den
        db [ i ] = hp*den
        c [ i ] = ho*den

    if (2*ns<n-m):
        dy = c [ ns+1 ]
    else:
        dy = db [ ns ]
        ns = ns-1
    y = y+dy

tau [m] = y ## This is where waiting time is calculated

t_sum = t_fin
    quit = True
else:
    t_sum = t_sum+tau [m]

if (t_sum>t_fin ):
    t_sum = t_fin
    quit = True
sn_ss = t_sum/delta_t
n_ss = int (sn_ss)
if (sn_ss != 0.0 and sn_ss-n_ss <0.5):
    n_ss = n_ss-1

```



```

elif (sn_ss==0.0):
    skip = True

for ntt in range(n_ss_old, n_ss+1):
    if (n_ss_old==0):
        wfn1 [nr, ntt, 1] = 1.0
        wfn1 [nr, ntt, 2] = 0.0
        wfn2 [nr, ntt, 1] = 0.0
        wfn2 [nr, ntt, 2] = 0.0
    else:
        wfn1 [nr, ntt, 1] = wfn1 [nr, n_ss_old, 1]
        wfn1 [nr, ntt, 2] = wfn1 [nr, n_ss_old, 2]
        wfn2 [nr, ntt, 1] = wfn2 [nr, n_ss_old, 1]
        wfn2 [nr, ntt, 2] = wfn2 [nr, n_ss_old, 2]
## Calculate the realizations of wave 1 #####
if (wfn1 [nr, ntt, 1]==0.0 and wfn1 [nr, ntt, 2]==0.0):
    wfn1_new [nr, ntt, 1] = 0.0
    wfn1_new [nr, ntt, 2] = 0.0
elif (wfn1 [nr, ntt, 1]==1.0 and wfn1 [nr, ntt, 2]==0.0):
    wfn1_new [nr, ntt, 1] = 1.0
    wfn1_new [nr, ntt, 2] = 0.0
## Calculate the realizations of wave 2 #####
if (wfn2 [nr, ntt, 1]==0.0 and wfn2 [nr, ntt, 2]==0.0):
    wfn2_new [nr, ntt, 1] = 0.0
    wfn2_new [nr, ntt, 2] = 0.0
elif (wfn2 [nr, ntt, 1]==0.0 and wfn2 [nr, ntt, 2]==1.0):
    wfn2_new [nr, ntt, 1] = 0.0
    wfn2_new [nr, ntt, 2] = 1.0
### Calculate the density matrix #####
rho [nr, ntt, 2, 2] = wfn1_new [nr, ntt, 2]**2

```

```

+ wfn2_new[nr, ntt, 2]**2
prodt[nr, ntt] = rho[nr, ntt, 2, 2]
if(skip):
    prodt[nr, 1] = 1.0
    break
if(quit):
    break
n_ss_old = n_ss+1
for i in range(1, 100+1):
    y = random.random()

rnn = random.random()
probgam=gamma1/(gamma1+gamma2)

if (rnn<probgam):
wfn1[nr, n_ss_old, 1] = 1.0
    wfn1[nr, n_ss_old, 2] = 0.0
    wfn2[nr, n_ss_old, 1] = 0.0
    wfn2[nr, n_ss_old, 2] = 0.0
else:
    wfn1[nr, n_ss_old, 1] = 0.0
    wfn1[nr, n_ss_old, 2] = 0.0
    wfn2[nr, n_ss_old, 1] = 0.0
    wfn2[nr, n_ss_old, 2] = 1.0
for i in range(0, s_n):
    prodt_total[i] = 0.0
    for j in range(1, nnr+1):
        prodt_total[i] = prodt_total[i]+prodt[j, i]
### Calculate the statistics #####
for i in range(0, s_n):

```

```

errt [ i ] = 0.0
ttt = i*delta_t+t_ini
for j in range(1,nnr+1):
    errt [ i ] = errt [ i ]+(prodt [ j , i ]-prodt_total [ i ]/nnr)**2
print i , ttt , prodt_total [ i ]/nnr , sqrt (errt [ i ]/(nnr*(nnr-1)))
txt = str(i) + '\t' + str(ttt) + '\t' + str(prodt_total [ i ]/nnr)
+ '\t' + str(sqrt (errt [ i ]/(nnr*(nnr-1)))) + '\n'
file . write (txt)

file . close ()

show ()
close ('all ')

if __name__ == "__main__":
    run ()
print ("---% seconds---"%(time . time () -start_time))

```

A.3 Weak coupling for correlated state

The same was used for the correlated state, but the initial conditions were different.

```

from qutip import *
from scipy import *
from pylab import *
import random
import time

start_time = time.time()
def run():
    n = 2

```

```
nnr = 5000
nt = 3000
tau = zeros([1500+1])
wfn1 = zeros((nnr+1,nt+1,n+1))
wfn2 = zeros((nnr+1,nt+1,n+1))
wfn1_new = zeros((nnr+1,nt+1,n+1))
wfn2_new = zeros((nnr+1,nt+1,n+1))
prodt = zeros((nnr+1,nt+1))
prodt_total = zeros((nt+1))
errt = zeros((nt+1))
rho = zeros((nnr+1,nt+1,n+1,n+1))

ira = 4321

N0 = 150
N1 = N0
N2 = N0
dlam = 0.001e00
dN1 = N1*1.0e00
dN2 = N2*1.0e00
d_e = 0.31
gamma1 = 2.0*pi*dlam**2*dN1/d_e
gamma2 = 2.0*pi*dlam**2*dN2/d_e
beta = 0.05e00

for i in range(1,nnr+1):
    for j in range(0,nt+1):
        prod_t[i,j]=0.0

for nr in range(1,nnr+1):
```

```
quit = False
skip = False
ira = ira+1
random.seed( ira )
rn = random.random()
t_ini = 0.0
t_fin = 5000.0
delta_t = 5.0
n_s = (t_fin-t_ini)/delta_t
s_n = int(n_s)
t_sum = 0.0
ntau_max = 100
n_ss_old = 0
tau[0] = 0.0

wfn1[nr, n_ss_old, 1] = 1.0
wfn1[nr, n_ss_old, 2] = 0.0
wfn2[nr, n_ss_old, 1] = 0.0
wfn2[nr, n_ss_old, 2] = 1.0

for m in range(1, ntau_max+1):
    quit = False
    skip = False

    rn = random.random()

    tau[m] = (-1.0/gamma1)*log(rn)

    if (tau[m]>t_fin):
```

```

        t_sum = t_fin
        quit = True
    else:
        t_sum = t_sum+tau [m]

    if (t_sum>t_fin):
        t_sum = t_fin
        quit = True
    sn_ss = t_sum/delta_t
    n_ss = int(sn_ss)
    if (sn_ss != 0.0 and sn_ss-n_ss < 0.5):
        n_ss = n_ss-1
    elif (sn_ss==0.0):
        skip = True

    for ntt in range(n_ss_old, n_ss+1):
        if (n_ss_old==0):
            wfn1 [nr, ntt, 1] = 1.0
            wfn1 [nr, ntt, 2] = 0.0
            wfn2 [nr, ntt, 1] = 0.0
            wfn2 [nr, ntt, 2] = 1.0
        else:
            wfn1 [nr, ntt, 1] = wfn1 [nr, n_ss_old, 1]
            wfn1 [nr, ntt, 2] = wfn1 [nr, n_ss_old, 2]
            wfn2 [nr, ntt, 1] = wfn2 [nr, n_ss_old, 1]
            wfn2 [nr, ntt, 2] = wfn2 [nr, n_ss_old, 2]

    if (wfn1 [nr, ntt, 1]==0.0 and wfn1 [nr, ntt, 2]==1.0):
        wfn1_new [nr, ntt, 1] = 0.0
        wfn1_new [nr, ntt, 2] = 1.0

```

```

wfn2_new [nr, ntt, 1] = 1.0
wfn2_new [nr, ntt, 2] = 0.0

else :
wfn1_new [nr, ntt, 1] = 1.0
wfn1_new [nr, ntt, 2] = 0.0
wfn2_new [nr, ntt, 1] = 0.0
wfn2_new [nr, ntt, 2] = 1.0

#rho [nr, ntt, 2, 2] = beta*wfn1_new [nr, ntt, 2]**2 + (1.0 e00
-beta)*wfn2_new [nr, ntt, 2]**2
#prodt [nr, ntt] = rho [nr, ntt, 2, 2]
rho [nr, ntt, 1, 2] = sqrt (beta*(1-beta))*(wfn1_new [nr, ntt
, 1]*wfn2_new [nr, ntt, 2])
prodt [nr, ntt] = rho [nr, ntt, 1, 2]
if (skip):
    prodt [nr, 1] = 1.0
    break
if (quit):
    break
n_ss_old = n_ss+1
if (wfn1 [nr, n_ss, 1]==0.0 and wfn1 [nr, n_ss, 2]==1.0):
wfn1 [nr, n_ss_old, 1] = 1.0
wfn1 [nr, n_ss_old, 2] = 0.0
wfn2 [nr, n_ss_old, 1] = 0.0
wfn2 [nr, n_ss_old, 2] = 1.0
else :
wfn1 [nr, n_ss_old, 1] = 0.0
wfn1 [nr, n_ss_old, 2] = 1.0
wfn2 [nr, n_ss_old, 1] = 1.0

```

```

wfn2[nr, n_ss_old, 2] = 0.0

for i in range(0, s_n+1):
    prodt_total[i] = 0.0
    for j in range(1, nnr+1):
        prodt_total[i] = prodt_total[i]+prodt[j, i]

for i in range(0, s_n+1):
    errt[i] = 0.0
    ttt = i*delta_t+t_ini
    for j in range(1, nnr+1):
        errt[i] = errt[i]+(prodt[j, i]-prodt_total[i]/nnr)**2
    print i, ttt, prodt_total[i]/nnr, sqrt(errt[i]/(nnr*(nnr-1)))
    txt = str(i) + '\t' + str(ttt) + '\t' + str(prodt_total[i]/nnr) + '\t' +
    file.write(txt)

#print gamma1, gamma2
file.close()

show()
close('all')

if __name__ == "__main__":
    run()
print ("---% seconds---"%(time.time() -start_time))

```

A.4 Strong coupling for correlated state

The same was used for the correlated state, but the initial conditions were different.


```
from qutip import *
from scipy import *
from pylab import *
import random
import time

start_time = time.time()
def run():
    n = 2
    nnr = 5000
    nt = 3000
    tau = zeros([1500+1])
    wfn1 = zeros((nnr+1,nt+1,n+1))
    wfn2 = zeros((nnr+1,nt+1,n+1))
    wfn1_new = zeros((nnr+1,nt+1,n+1))
    wfn2_new = zeros((nnr+1,nt+1,n+1))
    prodt = zeros((nnr+1,nt+1))
    prodt_total = zeros((nt+1))
    errt = zeros((nt+1))
    rho = zeros((nnr+1,nt+1,n+1,n+1))
    tt = zeros((10001+1))
    rnu = zeros((10001+1))
    t_t = zeros((5+1))
    rnuu = zeros((5+1))

    ira = 200

    N0 = 150
    N1 = N0
```

```

N2 = N0
dlam = 0.01e00
dN1 = N1*1.0e00
dN2 = N2*1.0e00
d_e = 0.31
gamma1 = 2.0*pi*dlam**2*dN1/d_e
gamma2 = 2.0*pi*dlam**2*dN2/d_e
beta = 0.050e00
for i in range(0,10000+1):
    tt[i] = 0.5*i*pi/180.0
    b = d_e*tt[i]
    a = 0.0*pi/180.0
    xm = 0.5*(b+a)
    xr = 0.5*(b-a)
    ee = d_e/2.0
    w = zeros((5))
    x = zeros((5))
    w = [0,0.2955242274, 0.2692667193, 0.2190863625
, 0.1494513491, 0.0666713443]
    x = [0,0.1488743389, 0.4333953941, 0.6794095682
, 0.8650633666, 0.9739065285]
    ss = 0.0
    for j in range(1,5+1):
        dx = xr*x[j]
        ss = ss+w[j]*(sin(xm+dx)/(xm+dx)+sin(xm-dx)/(xm-dx))
    ss = xr*ss
    tt[i] = 0.5*i*pi/180.0
    h = (-1+cos(d_e*tt[i])+d_e*tt[i]*ss)/(d_e*tt[i]*pi)
    rnu[i] = exp(-h*tt[i]*gamma1*2)
    rnu[0] = 1.0

```

```
for i in range(1, nnr+1):
    for j in range(0, nt+1):
        prodt[i, j]=0.0

for nr in range(1, nnr+1):

    quit = False
    skip = False
    ira = ira+1
    random.seed( ira )
    rn = random.random()
    t_ini = 0.0
    t_fin = 100.0
    delta_t = 0.1
    n_s = (t_fin-t_ini)/delta_t
    s_n = int(n_s)
    t_sum = 0.0
    ntau_max = 100
    n_ss_old = 0
    tau[0] = 0.0

    wfn1[nr, n_ss_old, 1] = 1.0
    wfn1[nr, n_ss_old, 2] = 0.0
    wfn2[nr, n_ss_old, 1] = 0.0
    wfn2[nr, n_ss_old, 2] = 1.0

    for m in range(1, ntau_max+1):
        quit = False
        skip = False
```

```
rn = random.random()

for ii in range(0,8500+1):
    if(rn<rnu[ii-1] and rn>rnu[ii]):
        break
for j in range(0,5+1):
    t_t[j]=tt[ii-1+j]
    rnuu[j]=rnu[ii-1+j]
if(t_t[0]>t_fin):
    tau[m] = t_t[0]

if(t_t[0]>t_fin):
    break
nmaxx = 10
n = 5
xa = rnuu
ya = t_t
c = zeros((nmaxx))
db = zeros((nmaxx))
ns = 1
x = rn
dif = abs(x-xa[1])

for i in range(1,n+1):
    dift = abs(x-xa[i])
    if (dift<dif):
        ns = i
        dif = dift
```

```
c[i] = ya[i]
db[i] = ya[i]

y = ya[ns]
ns = ns - 1

for m in range(1, (n-1)+1):
    for i in range(1, (n-m)+1):
        ho = xa[i]-x
        hp = xa[i+m]-x
        w = c[i+1]-db[i]
        den = ho-hp
        if (den==0.0):
            break
        den = w/den
        db[i] = hp*den
        c[i] = ho*den

    if (2*ns<n-m):
        dy = c[ns+1]
    else:
        dy = db[ns]
        ns = ns-1
    y = y+dy

tau[m] = y

if (tau[m]>t_fin):
    t_sum = t_fin
    quit = True
```

```

else :
    t_sum = t_sum+tau [m]

if (t_sum>t_fin ):
    t_sum = t_fin
    quit = True
sn_ss = t_sum/delta_t
n_ss = int (sn_ss)
if (sn_ss != 0.0 and sn_ss-n_ss <0.5):
    n_ss = n_ss-1
elif (sn_ss==0.0):
    skip = True

for ntt in range(n_ss_old , n_ss+1):
    if (n_ss_old==0):
        wfn1 [nr , ntt , 1] = 1.0
        wfn1 [nr , ntt , 2] = 0.0
        wfn2 [nr , ntt , 1] = 0.0
        wfn2 [nr , ntt , 2] = 1.0
    else :
        wfn1 [nr , ntt , 1] = wfn1 [nr , n_ss_old , 1]
        wfn1 [nr , ntt , 2] = wfn1 [nr , n_ss_old , 2]
        wfn2 [nr , ntt , 1] = wfn2 [nr , n_ss_old , 1]
        wfn2 [nr , ntt , 2] = wfn2 [nr , n_ss_old , 2]

if (wfn1 [nr , ntt , 1]==0.0 and wfn1 [nr , ntt , 2]==1.0):
    wfn1_new [nr , ntt , 1] = 0.0
    wfn1_new [nr , ntt , 2] = 1.0
    wfn2_new [nr , ntt , 1] = 1.0
    wfn2_new [nr , ntt , 2] = 0.0

```

```

else :
    wfn1_new [nr , ntt , 1] = 1.0
    wfn1_new [nr , ntt , 2] = 0.0
    wfn2_new [nr , ntt , 1] = 0.0
    wfn2_new [nr , ntt , 2] = 1.0

#rho [nr , ntt , 2 , 2] = beta*wfn1_new [nr , ntt , 2]**2 + (1.0 e00
-beta)*wfn2_new [nr , ntt , 2]**2
#prodt [nr , ntt] = rho [nr , ntt , 2 , 2]
rho [nr , ntt , 1 , 2] = sqrt (beta*(1-beta))*(wfn1_new [nr , ntt
, 1]*wfn2_new [nr , ntt , 2])
prodt [nr , ntt] = rho [nr , ntt , 1 , 2]
if (skip):
    prodt [nr , 1] = 1.0
    break
if (quit):
    break
n_ss_old = n_ss+1
for i in range (1,100+1):
    y = random.random()

rnn = random.random()
probgam=gamma1/(gamma1+gamma2)

if (rnn<probgam):
    wfn1 [nr , n_ss_old , 1] = 1.0
    wfn1 [nr , n_ss_old , 2] = 0.0
    wfn2 [nr , n_ss_old , 1] = 0.0
    wfn2 [nr , n_ss_old , 2] = 1.0

```

```

        else:
            wfn1[nr, n_ss_old, 1] = 0.0
            wfn1[nr, n_ss_old, 2] = 1.0
            wfn2[nr, n_ss_old, 1] = 1.0
            wfn2[nr, n_ss_old, 2] = 0.0

for i in range(0, s_n):
    prodt_total[i] = 0.0
    for j in range(1, nnr+1):
        prodt_total[i] = prodt_total[i]+prodt[j, i]

for i in range(0, s_n):
    errt[i] = 0.0
    ttt = i*delta_t+t_ini
    for j in range(1, nnr+1):
        errt[i] = errt[i]+(prodt[j, i]-prodt_total[i]/nnr)**2
    print i, ttt, prodt_total[i]/nnr, sqrt(errt[i]/(nnr*(nnr-1)))
    txt = str(i) + '\t' + str(ttt) + '\t' + str(prodt_total[i]/nnr) + '\t' +
    file.write(txt)

file.close()

show()
close('all')

if __name__ == "__main__":
    run()
print ("---% seconds---"%(time.time() -start_time))

```


Bibliography

- [1] M. Moodley and F. Petruccione. *Phys. Rev. A* **79** (2009) 042103.
- [2] M. Moodley, S. Paul, and T. Nsio Nzundu. *Phys.* **85** (2012) 045002.
- [3] E.B. Davies, *Quantum Theory of Open Systems*, Academic Press New York, London. (1976).
- [4] H.P. Breuer, F. Petruccione. *The Theory of Open Quantum Systems*, Oxford University Press, Oxford, (2002).
- [5] H. Carmichael. *An Open Systems Approach to Quantum Optics*, Springer-Verlag, New York, (1993).
- [6] Alicki. R., and Fannes. M. *Quantum Dynamical Systems*. Oxford University Press, Oxford, (2001).
- [7] G. Lindblad, *Commn. Math. Phys.* **48** (1976) 119.
- [8] V. Gorini, A. Kossakowski, and E. Sudarshan, *J. Math. Phys.* **17** (1976) 821.
- [9] E.B. Davies, *Commn. Math. Phys.* **39** (1974).
- [10] H.P Breuer. *Phys. Rev. A* **75** (2007) 022103.
- [11] H.P. Breuer, J. Gemmer, and M. Michel. *Phys. Rev. E* **73** (2006) 016139.
- [12] J. Gemmer and M. Michel, *Physica E* **29** (2005) 136.
- [13] X. L. Haung and X. X. Yi, *EPL* **82** (2005) 50001.

-
- [14] M. Esposito and Gaspard. *Phys. Rev. E* **68** (2003) 066112.
- [15] M. Esposito and Gaspard. *Phys. Rev. E* **68** (2003) 066113.
- [16] S. Nakajima. *Prog. Theor. Phys.* **20** (1958) 948.
- [17] R. Zwanzig, *J. Chem. Phys.* **33** (1960) 1338.
- [18] F. Shibata, Y. Takahashi, and N. Hashitsume, *J. Stat. Phys.* **17** (1977) 171.
- [19] W.H. Press, S.A. Teukolsky, W.T. Vetterling, and B.P. Flannery. *Numerical Recipes*. (2007).